ANALYSIS OF SOME SOLAR SYSTEM DYNAMICS PROBLEMS

Part 1: Some Implications of the Yarkovsky Effect

on the Orbits of Very Small Asteroids

Part 2: Stable Retrograde Orbits Outside the

Sphere of Influence

by

CHARLES ALAN PETERSON

B.S., M.I.T., 1966

M.S., M.I.T., 1966

SUBMITTED IN PARTIAL FULFILLMENT

OF THE REQUIREMENTS FOR THE

DEGREE OF DOCTOR OF PHILOSOPHY

at the

MASSACHUSETTS INSTITUTE OF TECHNOLOGY

May, 1976

Signature of Author _____
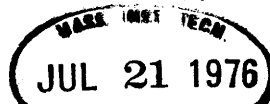
Department of Earth and Planetary Sciences

Certified by _____

Thesis Supervisor

Accepted by _____

Chairman, Departmental Committee
on Graduate Students

Analysis of Some Solar System Dynamics Problems

Part 1: Some Implications of the Yarkovsky Effect
on the Orbits of Very Small Asteroids

Part 2: Stable Retrograde Orbits Outside the
Sphere of Influence

by Charles Peterson

Abstract

Part I

Some previous difficulties associated with attributing an asteroid belt origin to meteorites are briefly reviewed. In order to overcome these difficulties, a two-step mechanism is proposed by which the small fragments produced by asteroid collisions are gradually sent into eccentric earth crossing orbits while the larger parent bodies themselves remain relatively unaffected. Central to this mechanism is the Yarkovsky effect, which arises from the asymmetric reradiation emitted by an illuminated rotating body. Due to thermal lags, the "evening" hemisphere of such a body will always be warmer on the average then the "morning" hemisphere. Not only can the Yarkovsky effect be three orders of magnitude greater than the well-known Poynting-Robertson drag, but unlike the latter, the Yarkovsky acceleration can be either positive or negative depending upon the sense of the body's rotation. The second stage of the proposed mechanism becomes important only when either of these two secular

accelerations succeeds in causing the orbital elements of the body to evolve into a secular resonance with Jupiter. There is some evidence that such transient resonances with Jupiter, brought about by the Yarkovsky effect, are responsible for the rather large orbital eccentricities observed for most meteorites. The Yarkovsky acceleration is explicitly calculated for both cylindrical and spherical bodies. When the orbital consequences of the Yarkovsky acceleration acting alone upon small asteroid belt fragments are determined, the results are found to be reasonably consistent with both the relative and absolute cosmic ray exposure ages of stony and iron meteorites.

Part II

The usual concept of the sphere of influence is violated by the retrograde orbit of Palomar-Leiden Survey object number 7617 about Jupiter. An analytic investigation of this orbit is presented. First Hill's equations for the sun-Jupiter system are used in the limit of zero secondary mass to demonstrate the existence of a class of distant retrograde variation orbits about Jupiter. It is then shown by two-body perturbation analysis that Jupiter's gravitational influence stabilizes this variation orbit, and some of the associated characteristic motions are explored. A comparison of the analytic results with a numerical integration of Hill's equations shows good agreement at large distances (>1 A.U.) from Jupiter. However, because of its large heliocentric eccentricity ($e \simeq 0.65$), the orbit of Palomar-Leiden object 7617

3

is not well described by Hill's equations. Nonetheless, the

investigation does provide a good heuristic explanantion for the

stability of this retrograde motion.

Thesis supervisor: Irwin I. Shapiro
                     Professor of Geophysics and Physics

Acknowledgments

Preface

The first part of this thesis deals quantitatively with the Yarkovsky effect as a possible means for the orbits of small (1-100 meters) asteroid fragments to gradually evolve into earth-crossing trajectories. Although first proposed by a Polish civil engineer more than 70 years ago and based upon sound physical principles, the Yarkovsky effect still remains rather obscure in the minds of most workers in the planetary sciences. In fact, had the author not independently rediscovered the effect for himself in the course of explaining the unexpected behavior of a laboratory experiment, he probably would have continued to remain unimpressed with its potential implications. It is hoped that this work will help in the future to heighten an awareness of the Yarkovsky effect in the minds of planetary investigators.

The second part of this thesis challanges the conventional concept of the "sphere of influence". It is shown that there is a continuum between distant retrograde orbits and one-to-one orbital resonance. The analytic approach used in this part is original with the author, and it is hoped that the approximate model upon which it is based succeeds in making the surprising stability of this motion comprehensible to the reader in an intuitive way.

Analysis of Some Solar System Dynamics Problems

Table of Contents

Part II

I. Introduction

For nearly two centuries science has accepted the fact that
cosmic debris occasionally falls onto the earth as meteorites.
This unquestionably extraterrestrial material has long been the
object of intense mineralogical study, and the maturing of atomic
physics during this century has made possible many types of
sophisticated analysis from which, among other things, the "age"
of the material can be deduced. Such studies have already pro-
vided both considerable insight into the chronology of the solar
system and valuable clues into its early physical state (Anders,
1971a,b). More recently, laboratory spectral reflectance
measurements of some meteorites have been shown to closely
resemble the spectral reflectances of some asteroids (McCord and
Gaffey, 1974; Chapman et al, 1975), thus adding to the circum-
stantial evidence that the asteroid belt is an important, if not
the major, source of meteorites. But there have always been
severe difficulties in explaining how fragments heavier than a
kilogram which are generated by asteroid collisions (Dohnanyi,
1971) can efficiently enter the inner solar system (Wetherill,
1969, 1971, 1974).

A. The Problem

The well known Poynting-Robertson effect is capable of
causing the orbital decay and eventual passage through the inner
solar system of all asteroid fragments smaller than about 10
centimeters. However, such fragments would be too small to

survive atmospheric entry, and most fragments large enough to survive entry and reach the earth's surface would be too big (i.e. would have too large a ratio of mass to surface area) for this mechanism to affect them significantly during the 4.6 billion year age of the solar system. So although the Poynting-Robertson effect undoubtedly influences both the distribution of solar system dust particles and many of the objects which are seen as meteors in the night sky, it probably cannot account for any meteorites recovered on the earth's surface that might have originated in the asteroid belt.

Neither is it likely that the collision process itself could impart enough of a velocity change for a resulting asteroid fragment to directly enter an earth crossing orbit. Although many meteorites display clear signs of shock which could indicate a violent collision in their past histories (Wasson, 1974), all meteorite classes contain a significant number of members which display no evidence of shock. Studies of the cratering process have shown that the highest velocity ejecta tend to be broken up into the smallest fragments, and that most of the larger fragments are ejected at less than 1 km/sec (Gault et al, 1963). Since a 5 km/sec velocity change is needed within the asteroid belt to enter an earth crossing orbit, it seems improbable that many fragments large enough to survive earth atmospheric entry could result from such a mechanism. In fact, even if we remain entirely within the earth's gravitational sphere of influence where only a 3 km/sec velocity change would be necessary to enable lunar crater

ejecta to reach the earth, we find that there is as yet not one recovered meteorite that is known to have come from the moon (Wetherill, 1974).

Various orbital resonances of asteroid fragments with the major planets, principally Jupiter, are sometimes invoked to explain how meteorites enter the inner solar system. Indeed this concept has gained new support with the recent discovery that both the Lost City and Pribram bodies were undergoing very rapid secular changes in their orbital elements just prior to their entering the earth's atmosphere (Lowery, 1971; Williams, 1972). However, it does not seem to be generally recognized that there are two serious difficulties with this mechanism when considered in its simplest form. First the cosmic ray exposure ages of most stony meteorites indicate that the separation events from their parent bodies occurred more than 4 million years ago while the rates of orbital evolution due to Jovian resonances are so great that only about one million years are necessary to bring their orbits into the inner solar system (Williams, 1973). It would be as though the fragments were content to orbit uneventfully within the asteroid belt for most of their lives as free bodies and then were abruptly removed from the belt by Jovian perturbations during the last quarter of their lives. The implausibility of this scenario would become even more pronounced for iron meteorites which have cosmic ray exposure ages typically fifty times greater than those for stones. The second difficulty results from the fact that gravity perturbations produce acceler-

ations independent of density, size, or physical properties. If Jupiter can perturb small fragments within tens or hundreds of millions of years and send them into earth crossing orbits, then why couldn't it do the same thing to the larger asteroids from which the fragments originated during the 4.6 billion year age of the solar system? The typical orbits of the fragments could not be expected to be significantly different from that of the asteroid source. It has been noted that both the Lost City and Pribram meteorites were in secular resonances with Jupiter (Williams, 1972, 1975), and perhaps this fact points toward a <u>combination</u> of effects comprising a multistep mechanism which somehow must act more efficiently upon the small fragments than upon the asteroids themselves.

The evidence we have so far indicates that the final step in the source mechanism for meteorites may involve gravitational resonances (a nonselective process), therefore, <u>as a candidate for the next-to-last step</u>, $\wedge$ consider the effect of the well-known Poynting-Robertson drag on a small fragment in the same orbit as its much larger asteroid parent body. Because "light pressure" forces accelerate bodies of the same density in direct proportion to their surface areas and in inverse proportion to their volumes, the Poynting-Robertson drag will act <u>selectively</u> on the orbit of the small fragment and cause it to evolve more rapidly. By itself, this process would cause a continuous decrease in both the semimajor axis and orbital eccentricity until the small body either collided with a planet or was vaporized close to the sun. However, it has been

12

previously observed that in the course of its journey from the asteroid belt to the inner solar system, such a body would have to traverse the Kirkwood gaps and perhaps would encounter various other resonance phenomena as well (Peterson, 1975). Evidence that such complications on the orbital dynamics of small solar system bodies actually do occur will be discussed later. Unfortunately, the Poynting-Robertson effect is too weak for even this scenario to work as a source mechanism for meteorites within the time constraints imposed by cosmic ray exposure age measurements. However, a largely ignored phenomenon known as the Yarkovsky effect does seem capable of explaining most of the dynamical data on meteorites (Peterson, 1975). Although it is also a (selective) light pressure type of force, the Yarkovsky effect can be a few orders of magnitude greater than the Poynting-Robertson effect as we shall soon see.

B. The Yarkovsky Effect

According to Öpik (1951), a Polish Civil Engineer named Yarkovsky* published a paper in Russian about 1900 proposing that the anisotropic thermal reradiation from a rotating body in solar orbit could have a significant long term effect on that orbit. He suggested that because of thermal lags, the "evening hemisphere" (see figure 1) of a rotating body will always be warmer on the average than the "morning hemisphere". The T^4 radiation law will then require that more thermal energy be emitted from the evening

*This name also appears as "J. Yarkovski" in a French language publication of 1888.

hemisphere and consequently more electromagnetic momentum flux
as well. This will result in a force imbalance in a direction
perpendicular to that of the incident radiation. It is the
production of this net transverse force on the rotating body that
we shall call the Yarkovsky effect. Of course, much of the
anisotropic reemission of electromagnetic momentum will be in the
direction of the sun and thus only serve to increase the outward
radial force on the body already incurred when the light energy
was first absorbed. But as long as both gravity and the radial
component of light pressure vary as the inverse square of the
distance, the net result of the two forces acting together may
be treated by simply modifying the effective gravity constant of
the sun. Unlike these purely radial forces, which do no net work
on the body during a complete orbit, the Yarkovsky force can have
a steady transverse component parallel to the orbital velocity
vector, and thus do net work over an orbital period, thereby
causing significant secular changes in the semimajor axis.

The only direct reference to Yarkovsky's work of which the
author is aware was made from memory by Öpik in 1951. In the
course of an enlightening quantitative comparison of the Poynting-
Robertson and Yarkovsky effects, Öpik simply stated that he had
read Yarkovsky's paper sometime around 1909. A year later
Radzievsky (1952) considered the effect, and he treated the quan-
titative aspects of the problem more rigorously. Jacchia (1963)
referred to both Öpik's and Radzievsky's papers, but remained
noncommital as to the actual significance of the effect. In 1965

14

the author independently rediscovered the effect while working
at the MIT Center for Space Research on methods of passive
attitude control for small spacecraft. The application of the
effect to asteroids and meteoroids was recognized at the time but
not exploited; however, a quantitative mathematical analysis of
the Yarkovsky effect was the central topic of the author's Mas-
ter's thesis (Peterson, 1966).

In order to properly assess the significance of the Yarkovsky
effect operating in the region of the asteroid belt, a quantita-
tive treatment is necessary. First we calculate the temperature
distribution on a rotating cylinder receiving solar illumination,
and thereby obtain an analytic expression for the reradiation
forces as a function of illumination intensity, cylinder physical
properties, and spin rate. Although only a linearized approxim-
ation to this problem is actually obtained in the text, some
mathematical ground work is laid out for a more extensive non-
linear treatment using analytic methods in Appendix A. The
results for the reradiative forces on a cylinder may first be
generalized to a cone and then applied to each differential
"slice" of a sphere. When this expression is integrated, there
emerge simple analytic relationships which may be used to cal-
culate explicity in two dimensions the effects of reradiation
forces on the orbital parameters of the sphere. A numerical
example is used both to help compare the Yarkovsky and Poynting-
Robertson effects and to acquaint the reader with the rates of

orbital evolution characteristic of the Yarkovsky effect acting upon meteorite-sized bodies. Finally, an attempt is made to correlate various dynamical data on meteorites to what might be expected from the source mechanism proposed in this work.

II. The Temperature Distribution on a Rotating Cylinder

A. The Basic Equations

Consider a cylinder of radius R whose axis is perpendicular to the incident solar radiation of intensity I_0. As the cylinder rotates at angular velocity ω, let $\psi = \omega t$ represent the angular position of a cylindrical element with respect to "local sunrise" as shown in figure 1. If conditions allow us to neglect circumferential heat conduction, which would certainly be the case for a large body, and we let r represent the depth into the body as measured from its surface inward, then the one dimensional heat flow equation determines the temperature, T(r,t) within the cylinder as

$$\frac{\partial T(r,t)}{\partial t} = k \frac{\partial^2 T(r,t)}{\partial r^2} \qquad\qquad k = \frac{K}{\rho C_p} \qquad\qquad (1)$$

where k is the thermal diffusivity, K is the thermal conductivity, C_p is the heat capacity, ρ is the density, and t is the time. Because the environmental conditions here determine the heat flux at the cylinder surface and not the actual temperature itself, the surface boundary condition on equation (1) takes the form of an energy conservation statement for r = 0 which may be written as

$$K \left. \frac{\partial T(r,t)}{\partial r} \right|_{r=0} = \epsilon \sigma T^4(0,t) - \alpha I(t) \qquad\qquad (2)$$

where the net heat loss from a cylinder element is attributed to the well-known T^4 thermal radiation law less the solar heat which

17
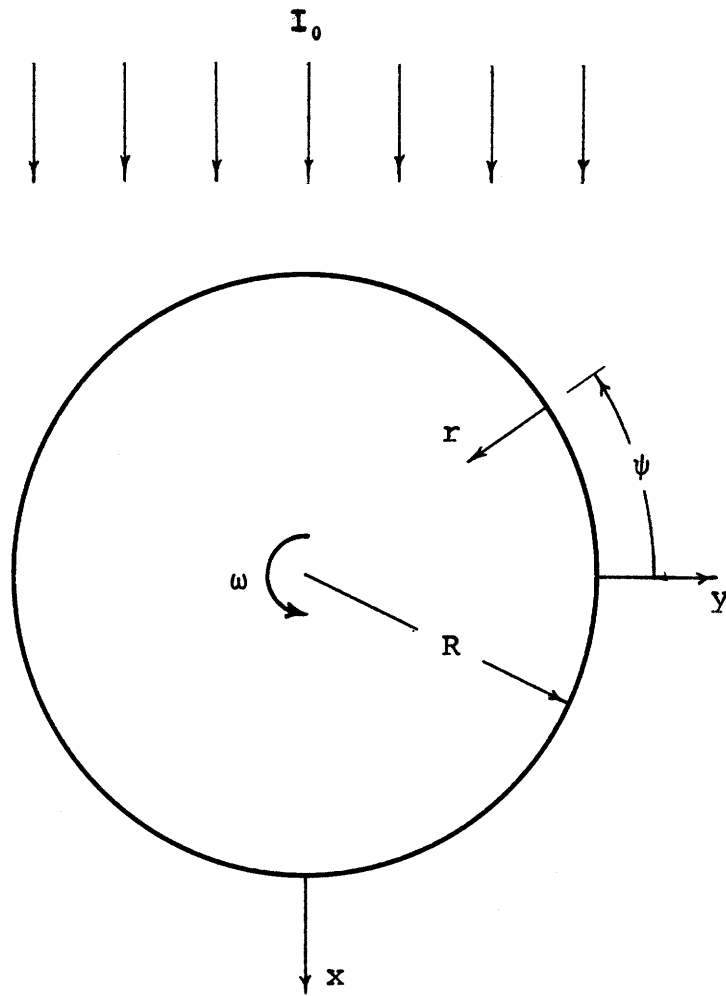
Figure 1

The coordinate system used in treating the problem of the
temperature distribution on an illuminated rotating cylinder.
The spin axis is assumed to be perpendicular to the orbital
plane, which is defined by the x and y coordinates as shown.

the element absorbs. Here α is the surface absorptivity, ε is
the surface emissivity, σ is the Stefan-Boltzmann constant, and
$I(t)$ is the solar flux which a cylinder element experiences as a
function of time, which will have the form of a half-rectified
sinusoid of amplitude I_0 and whose Fourier series is given by

$$I(t) = I_0 \left(\frac{1}{\pi} + \frac{\sin \omega t}{2} - \frac{2}{\pi} \sum_{n=1}^{\infty} \frac{\cos 2n\omega t}{4n^2 - 1} \right). \tag{3}$$

B. Steady State

An enormous, yet justifiable, simplification of the general
problem results if we assume that the temperature distribution
within the cylinder has already reached its steady state value
independent of the initial conditions. This means that the
cylinder as a whole is not heating up or cooling off and also
that every element radiates away exactly as much heat as it ab-
sorbs during each cycle. (Except possibly for the case of large
bodies in rather eccentric orbits, transients would not be of
interest here anyway.) This in turn means that even though the
temperature profile beneath each cylinder element changes with
time, it is always exactly the same for any element as it reaches
a given fixed value of the rotation angle, ψ. Another way of
looking at this is that while the cylinder itself rotates with
respect to the sun, the temperature distribution within it does
not. This situation allows us to use ψ and ωt interchangeably in
what follows.

The most general solution to equation (1) which can result from the periodic driving term given by equation (3) and satisfy the assumption of steady state can be written as

$$T(r,t) = T_0\left[1 + \sum_{n=1}^{\infty} A_n(r) \sin n\omega t + \sum_{n=1}^{\infty} B_n(r) \cos n\omega t \right]. \qquad (4)$$

When this equation is substituted into equation (1) and the coefficient of each periodic term is required to vanish, we get two coupled ordinary differential equations

$$-n\omega B_n = k\frac{d^2 A_n}{dr^2} \qquad n\omega A_n = k\frac{d^2 B_n}{dr^2} \qquad n = 1,2,3,4,\ldots\ldots$$

whose solution is readily found to involve a growing and decaying exponential for both A_n and B_n. However, if it is assumed that the cylinder is "large", then we may safely deduce that the steady state temperature fluctuations will certainly not grow exponentially with r as we approach the cylinder's center. This interior boundary condition thus permits us to reject the growing exponential which leaves

$$A_n(r) = e^{-\sqrt{n}\lambda r}\left(v_n \sin\sqrt{n}\lambda r + u_n \cos\sqrt{n}\lambda r \right)$$

$$B_n(r) = e^{-\sqrt{n}\lambda r}\left(-u_n \sin\sqrt{n}\lambda r + v_n \cos\sqrt{n}\lambda r \right)$$

$$(5)$$

where $\lambda = \sqrt{\omega/2k}$ and v_n and u_n are the two remaining arbitrary constants of integration which must be determined from the surface boundary condition (2). A "large" cylinder is now defined after Öpik (1951) as one for which $\lambda R > 4$, and this criterion is seen to depend upon spin rate and thermal diffusivity as well as upon the actual cylinder radius.

20

When equation (5) is substituted into (4) and the result is used to evaluate the left hand side of equation (2), we get for the net heat flux through the cylinder surface

$$K \left. \frac{\partial T(r,\psi)}{\partial r} \right|_{r=0} = KT_0 \lambda \sum_{n=1}^{\infty} \sqrt{n} \left[(v_n - u_n) \sin n\psi - (u_n + v_n) \cos n\psi \right] \quad (6)$$

where the steady state assumption has permitted us to replace ωt by ψ. Now because of the nonlinear nature of the radiation boundary condition, it is no longer convenient to write general expressions for the nth fourier term. Therefore, only second order terms up through the third harmonic will be retained from now on with each v_n and u_n considered to be first order. (It is shown in Appendix A that all higher odd harmonic terms are actually third order quantities.) Thus substituting equations (5) into (4) and evaluating the result at $r = 0$ we get for the surface temperature

$$T(0,\psi) = T_0 \left(1 + u_1 \sin \psi + v_1 \cos \psi + u_2 \sin 2\psi \right.$$
$$\left. + v_2 \cos 2\psi + u_3 \sin 3\psi + v_3 \cos 3\psi \right) \quad (7)$$

and raising this equation to the fourth power yields

$$T^4(0,\psi) = T_0^4 \left(1 + \delta + U_1 \sin \psi + V_1 \cos \psi + U_2 \sin 2\psi \right.$$
$$\left. + V_2 \cos 2\psi + U_3 \sin 3\psi + V_3 \cos 3\psi \right) \quad (8)$$

where we have defined:

21

$$\delta(u_n, v_n)^* = 3\left(u_1^2 + v_1^2 + u_2^2 + v_2^2 + u_3^2 + v_3^2 \right)$$

$$U_1(u_n, v_n) = 4u_1 + 6\left(v_1 u_2 - u_1 v_2 - u_2 v_3 + v_2 u_3 \right)$$

$$V_1(u_n, v_n) = 4v_1 + 6\left(u_1 u_2 + v_1 v_2 + u_2 u_3 + v_2 v_3 \right)$$

$$U_2(u_n, v_n) = 4u_2 + 6\left(u_1 v_1 - u_1 v_3 + v_1 u_3 \right) \tag{9}$$

$$V_2(u_n, v_n) = 4v_2 + 3\left(v_1^2 - u_1^2 \right) + 6\left(u_1 u_3 + v_1 v_3 \right)$$

$$U_3(u_n, v_n) = 4u_3 + 6\left(u_1 v_2 + v_1 u_2 \right)$$

$$V_3(u_n, v_n) = 4v_3 + 6\left(v_1 v_2 - u_1 u_2 \right)$$

The many trigonometric cross products which result from raising equation (7) to the fourth power have been decomposed into their Fourier components and incorporated into the coefficients defined above.

All of the expressions necessary to apply the boundary condition (2) have now been evaluated in terms of their respective Fourier series. So if we substitute equations (3), (6), and (8) into equation (2) and then require that the resulting expression be an identity for all values of ψ, we will get seven equations in the seven unknowns T_0, u_1, v_1, u_2, v_2, u_3, v_3 as follows:

$$0 = \varepsilon \sigma T_0^4 (1 + \delta) - \alpha I_0/\pi$$

$$-KT_0 \lambda \left(u_1 - v_1 \right) = \varepsilon \sigma T_0^4 U_1 - \alpha I_0/2$$

$$-KT_0 \lambda \left(u_1 + v_1 \right) = \varepsilon \sigma T_0^4 V_1$$

$$-KT_0 \sqrt{2} \lambda \left(u_2 - v_2 \right) = \varepsilon \sigma T_0^4 U_2 \tag{10}$$

$$-KT_0 \sqrt{2} \lambda \left(u_2 + v_2 \right) = \varepsilon \sigma T_0^4 V_2 + 2\alpha I_0/3\pi$$

$$-KT_0 \sqrt{3} \lambda \left(u_3 - v_3 \right) = \varepsilon \sigma T_0^4 U_3$$

$$-KT_0 \sqrt{3} \lambda \left(u_3 + v_3 \right) = \varepsilon \sigma T_0^4 V_3$$

* Here we mean $u_n = \{u_1, u_2, u_3, \ldots\}$ and $v_n = \{v_1, v_2, v_3, \ldots\}$.

Next use the first of the above equations to eliminate the $\varepsilon\sigma T_0^4$
factor from the remaining six, and then multiply these resulting
equations by $\pi(1+\delta)/\alpha I_0$ to get

$$T_0^4 = \alpha I_0 \left[\varepsilon\sigma\pi(1+\delta)\right]^{-1} \tag{11a}$$

$$-P(1+\delta)\left(u_1 - v_1\right) = U_1 - (1+\delta)/2 \tag{11b}$$

$$-P(1+\delta)\left(u_1 + v_1\right) = V_1 \tag{11c}$$

$$-\sqrt{2}P(1+\delta)\left(u_2 - v_2\right) = U_2 \tag{11d}$$

$$-\sqrt{2}P(1+\delta)\left(u_2 + v_2\right) = V_2 + 2(1+\delta)/3 \tag{11e}$$

$$-\sqrt{3}P(1+\delta)\left(u_3 - v_3\right) = U_3 \tag{11f}$$

$$-\sqrt{3}P(1+\delta)\left(u_3 + v_3\right) = V_3 \tag{11g}$$

where we have defined

$$P = \pi K T_0 \lambda/\alpha I_0 = \frac{\pi T_0}{\alpha I_0 \sqrt{2}}\sqrt{\rho C_p K\omega}.$$

It is now our task to solve equations (11) for T_0, u_n, and v_n
remembering that $\delta = \delta(u_n, v_n)$, $U_n = U_n(u_n, v_n)$, and $V_n(u_n, v_n)$. The
more detailed treatment is reserved for Appendix A, however a
simplified version of the method yields results that not only
turn out to be quite accurate for large values of P, but which
also provide considerable insight into one nonlinear characteris-
tic of the exact solution.

C. An Approximate Steady State Solution

An approximate but useful solution to equations (11) can be
obtained by neglecting the second order terms in equations (11b -
11g). This permits us to ignore the third harmonic entirely since

23

$u_3 = 0 = v_3$ is then a solution to equations (11f) and (11g), and we have left;

$$T_0^4 = \alpha I_0 \left[\varepsilon \sigma \pi (1 + 3(u_1^2 + v_1^2 + u_2^2 + v_2^2)) \right]^{-1} \tag{12a}$$

$$-P(\, u_1 - v_1) = 4u_1 - \pi/2 \tag{12b}$$

$$-P(\, u_1 + v_1) = 4v_1 \tag{12c}$$

$$-\sqrt{2}P(\, u_2 - v_2) = 4u_2 \tag{12d}$$

$$-\sqrt{2}P(\, u_2 + v_2) = 4v_2 + 2/3. \tag{12e}$$

Since equations (12b) and (12c) are now decoupled from (12d) and (12e), we can immediately solve for u_1, v_1, u_2, and v_2 as

$$u_1 = \frac{\pi}{4}(P + 4)/(P^2 + 4P + 8) \tag{13a}$$

$$v_1 = -\frac{\pi}{4} P/(P^2 + 4P + 8) \tag{13b}$$

$$u_2 = -\frac{\sqrt{2}}{6}P/(P^2 + 2\sqrt{2}P + 4) \tag{13c}$$

$$v_2 = -\frac{1}{6}(\sqrt{2}P + 4)/(P^2 + 2\sqrt{2}P + 4) \tag{13d}$$

which expressions agree exactly with equations (15) of Radzievsky (1952) if his spin angle λ is replaced by our angle $\psi - \frac{\pi}{2}$ and his parameter ψ is replaced by our quantity $\frac{4}{P}$. In fact, because Radzievsky retained only linear terms in raising his counterpart of our equation (7) to the fourth power, he was able to express the general n^{th} fourier coefficient in equation (8) as $U_n = 4u_n$ and $V_n = 4v_n$; thus he could solve explicity for all u_n and v_n. This proceedure works quite well for "large" values of P, and it is one of the main purposes of Appendix A to show just where this linear approximation breaks down.

24

D. An Important Nonlinear Effect

One such source of breakdown is already discernible in equations (12) and (13). As long as ω is large, then P will be large, and u_n and v_n will be small. Thus equation (12a) shows that in such a case there will only be a very small effect of ω on T_0, even if we neglect u_n and v_n initially. However, once these values have been calculated from equations (13), then their effect in equation (12a) is to slightly reduce the original value of T_0, the new value of which we can then use to get an improved value for P in equations (13) and again solve for u_n and v_n if desired. A simple example can provide a clearer physical understanding of why the "average" temperature, T_0, should decrease nonlinearly with spin rate. Consider first a cylinder spinning so rapidly that the entire surface is virtually at the same temperature T_0. Under such circumstances the energy balance between the absorbed and emitted radiation may be written as

$$\epsilon \int_0^{2\pi} \sigma T_0^4 R d\psi = 2\alpha I_0 R, \qquad \text{or} \qquad \pi\epsilon\sigma T_0^4 = \alpha I_0.$$

Now imagine the spin slowed down until a perceptible temperature variation over the cylinder's surface appears which might be expressed approximately as

$$T(\psi) = T_0 (1 + u \sin \psi + v \cos \psi). \tag{14}$$

The corresponding energy balance now becomes (to second order)

$$\epsilon \int_0^{2\pi} \sigma T^4 (\psi) R d\psi \simeq \epsilon \int_0^{2\pi} \sigma T_0^4 \left(1 + 4(u \sin \psi + v \cos \psi)\right.$$

$$\left. + 6(u \sin \psi + v \cos \psi)^2\right) R d\psi = 2\alpha I_0 R$$

which reduces to

$$\pi\varepsilon\sigma T_0^4 \left(1 + 3u^2 + 3v^2\right) = \alpha I_0$$

whose T_0 must now be less than that for the previous situation involving only a uniform temperature distribution. What has happened here is that the T^4 radiation law causes a greater excess of heat to be radiated near the maximum value of $T(\psi)$ than is compensated for near its minimum value. Consequently, the "average" temperature, T_0, must be lowered to maintain an energy balance. Indeed, equation (11a) turns out to be equivalent to the condition that energy be conserved to second order. An important consequence of this fact is that linear treatments of this problem will always yield temperature distributions on the cylinder which radiate away more total heat than they absorb.

III. Thermal Reradiation Forces on a Rotating Cylinder

A. Analysis

Once we know the temperature distribution on the surface of a thermally radiating body, then it can be shown that if each element radiates according to the cosine law, the resulting force, $\vec{F}$, may be calculated by integrating

$$d\vec{F} = - \frac{2\varepsilon\sigma T^4}{3c} d\vec{S}$$

over the body's entire surface, where $d\vec{S}$ represents the outward normal to a differential surface element and c is the speed of light. In particular, the x and y components of this force may be evaluated by recognizing that $dS_x = - Rd\psi \cdot \sin \psi$ and $dS_y = Rd\psi \cdot \cos \psi$ respectively. Thus using T^4 as given by equation (8) we get for a cylinder of __unit__ __height__ (see figure 1)

$$F_x = \frac{2\varepsilon\sigma R}{3c} \int_0^{2\pi} T^4 (0,\psi) \sin \psi \, d\psi = \frac{2\varepsilon\sigma T_0^4}{3c} \pi R U_1$$

$$F_y = - \frac{2\varepsilon\sigma R}{3c} \int_0^{2\pi} T^4 (0,\psi) \cos \psi \, d\psi = - \frac{2\varepsilon\sigma T_0^4}{3c} \pi R V_1$$

where all harmonics other than the first have been eliminated by the orthogonality property of fourier series. Here it is a convenient notational coincidence that we may associate the quantity F_y with both the y component of the reradiative force and the Yarkovsky force because both of these designations happen to begin with the same letter. Next we use equation (11a) to eliminate the factor $\pi\varepsilon\sigma T_0^4$ from the above equations and then de-

fine $F_d = 2RI_0/c$ as the "direct" light pressure force or the magnitude of momentum intercepted by our cylinder of unit height to get

$$F_x = \frac{\alpha U_1}{3(1+\delta)} F_d \qquad (15a)$$

$$F_y = -\frac{\alpha V_1}{3(1+\delta)} F_d \; . \qquad (15b)$$

The quantity F_d represents the total electromagnetic momentum flux intercepted by the cylinder, and so the dimensionless ratio F_y/F_d is a measure of the efficiency with which this reradiation process produces a transverse force. In our momentum budget we explicitly ignore that portion of the incident energy which is not absorbed at the cylinder's surface (i.e. that portion which is specularly reflected or diffusely scattered). Rather than evaluating $U_1(u_n, v_n)$ and $V_1(u_n, v_n)$ from definition (9), it is more convenient to use equations (11b) and (11c) in equations (15) to get

$$F_x = \frac{\alpha F_d}{3} \left[\pi/2 - P(u_1 - v_1) \right] \qquad (16a)$$

$$F_y = \alpha F_d P(u_1 + v_1)/3 \qquad (16b)$$

where now all of the other u_n and v_n are only implicitly involved through the solution of the nonlinear coupled equations (11) for u_1 and v_1.

No approximations were made in obtaining equations (16); however, we are in a good position to gain some more insight into the nature of these reradiative force components by using the

28

approximations (13a) and (13b) in equations (16) to get

$$F_x = (\pi/3) \frac{P + 4}{P^2 + 4P + 8} \alpha F_d \qquad (17a)$$

$$F_y = (\pi/3) \frac{P}{P^2 + 4P + 8} \alpha F_d \qquad (17b)$$

which are graphed in figure 2. While F_x decreases monotonically with increasing P, the Yarkovsky force, F_y, is seen to have a maximum which can readily be determined by setting the derivative of equation (17b) to zero which yields

$$P\left(F_y = max \right) = \sqrt{8}^* \qquad (18a)$$

$$max\left(F_y \right) = \frac{\pi \alpha F_d}{12(1 + \sqrt{2})} \simeq 0.108 \ \alpha F_d. \qquad (18b)$$

Thus a large ($\lambda R > 4$) cylinder undergoing illumination at right angles to its axis of symmetry and rotating at just the optimum angular velocity can experience a transverse force (Yarkovsky force) which amounts to about 10% of the available incident momentum flux. Neither the fact that the Yarkovsky force would be maximized for some value of P nor the rather large values it could attain near this maximum seems to have been noticed by Radzievsky (1952). Instead he quickly replaced his equivalent of our equation (17b) with an asymptotic approximation valid for large P which is given in our notation by

$$F_y \simeq \frac{\pi \alpha F_d}{3P} \qquad P > 20 \qquad (19)$$

and which is depicted by the dashed line in figure 2.

* The linear approximations may not be very accurate for such a small value of P.

29
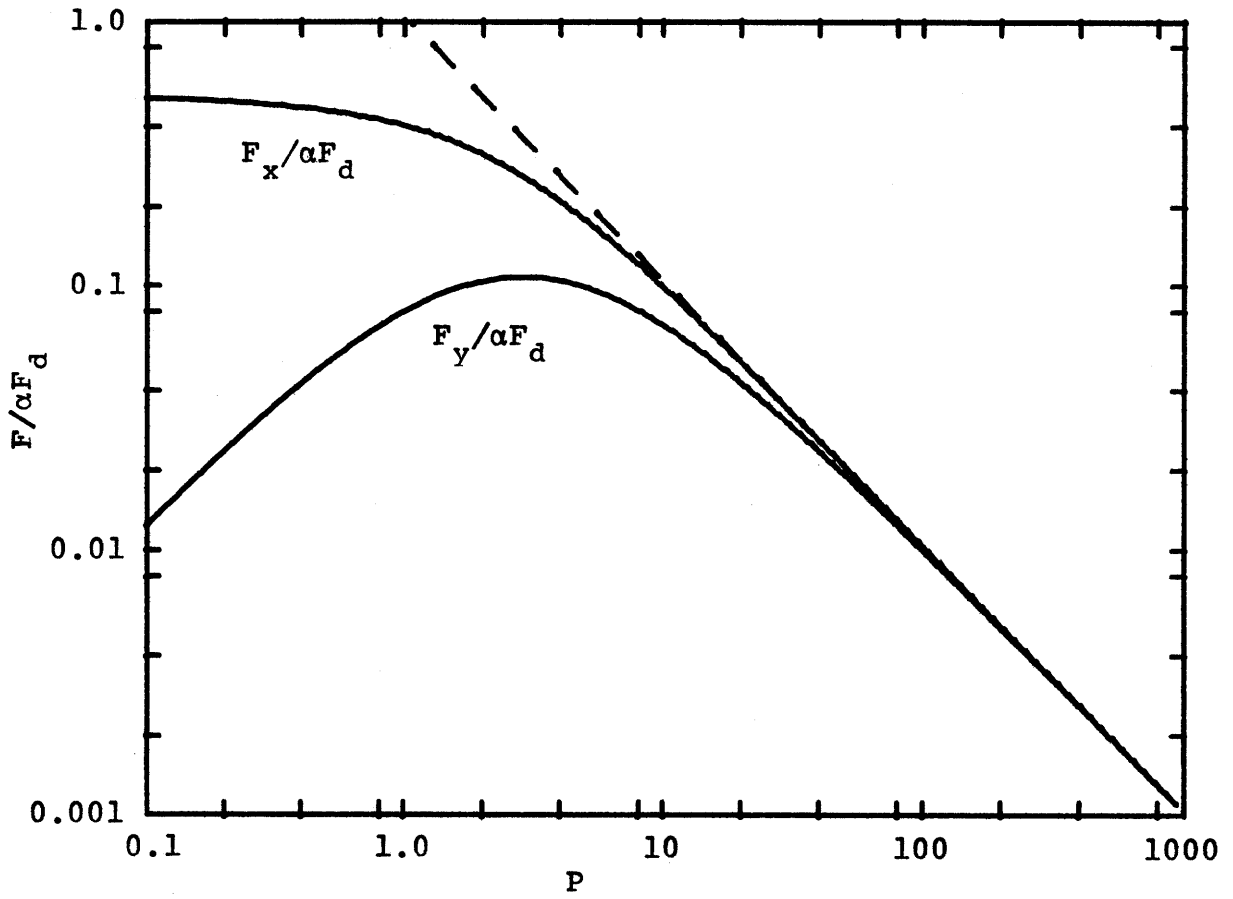
Figure 2

The x and y components of the reradiation force on an illuminated rotating cylinder expressed as a fraction of the "available" light pressure. Note that the Yarkovsky force can attain ten percent of this value at its maximum. The quantity α represents the cylinder's surface absorptivity while F_d may be regarded as the amount of incident electromagnetic momentum flux which is missing from the cylinder's shadow. The parameter P is given by

$$P = \frac{\pi T_0}{\alpha I_0} \sqrt{\frac{1}{2} \rho C_p K \omega} \ .$$

30

Although equation (19) is indeed satisfactory for the specific case which Radzievsky considered, note that it blows up for P = 0. On the other hand, it is not difficult to show that equations (17) actually attain the correct values of F_x and F_y for both P = 0 and P = ∞ as follows:

$$F_x(0) = (\pi/6)\alpha F_d$$
$$F_x(\infty) = F_y(0) = F_y(\infty) = 0.$$

For the Yarkovsky force, this is in accord with our intuition which demands that F_y vanish for a very rapidly spinning cylinder (P → ∞) as well as for a nonrotating cylinder (P = 0).

B. A Numerical Example

It is now appropriate to assess some of the implications of our calculations by considering a numerical example. Using Alexeyeva's (1958, 1960) measurements of the thermal properties for a number of meteorites, we may model a "typical" low-metal stony meteorite as follows;

$$\rho = 2.5 \text{ gm cm}^{-3}$$
$$C_p = 1.0 \times 10^7 \text{ erg } {}^0K^{-1} \text{gm}^{-1}$$
$$K = 1.5 \times 10^5 \text{ erg } {}^0K^{-1} \text{cm}^{-1} \text{sec}^{-1}.$$

Other physical parameters needed are

$$\sigma = 5.67 \times 10^{-5} \text{ erg } {}^0K^{-4} \text{cm}^{-2} \text{sec}^{-1}$$
$$I_0 = 1.4 \times 10^6 \text{ erg cm}^{-2} \text{sec}^{-1} \text{ at 1 Astronomical Unit}$$
$$\alpha = \epsilon = 1$$

from which we derive the following quantities using equation (11a)

with $\delta = 0$ and equation (18a)

$$T_0 = \left[\frac{I_0}{\sigma\pi}\right]^{1/4} = 298^\circ K$$

$$\omega\left(F_y = \max\right) = \frac{16I_0^2}{\pi^2 T_0^2 \rho C_p K} = 9.6 \times 10^{-6} \text{ radians/second}$$

where this optimum angular velocity corresponds to a rotation period of 183 hours. If we now choose a "typical" rotation rate of $\omega = 3.5 \times 10^{-4} \text{ sec}^{-1}$ corresponding to a period of about 5 hours, then we obtain from equations (5), (11), (17), and their associated definitions

$$\lambda = \sqrt{\frac{\rho C_p \omega}{2K}} = 0.17 \text{ cm}^{-1}$$

$$P = \frac{\pi T_0}{\alpha I_0 \sqrt{2}} \sqrt{\rho C_p K \omega} = 17.1$$

$$F_x = 0.060 \, \alpha F_d$$

$$F_y = 0.049 \, \alpha F_d.$$

The derived value for λ shows that the thermally conducting "skin depth" under these conditions is about 6 centimeters; that is, the diurnal temperature fluctuations are diminished in amplitude beneath the cylinder surface by a factor of e for every 6 centimeters of depth. Thus the criterion $\lambda R > 4$ means that the cylinder's radius, R, must exceed 24 centimeters in order for the assumption leading to equations (5) to be valid. The derived value for P, when compared to the optimum value of $\sqrt{8}$, shows that we are in the "fast" spin regime. Because the cylinder's surface absorptivity is assumed to be unity in this case, we see from the

32

value for F_y above that the Yarkovsky force still amounts to nearly 5% of all the available electromagnetic momentum flux in this non-optimal case. However, we should observe that this rather vigorous value for the Yarkovsky force would be substantially reduced by two separate effects if the cylinder were to be transported from 1 A.U. to the asteroid belt at 3 A.U. First the available incident momentum, F_d, would diminish by a factor of nine since the solar illumination obeys an inverse square law. Second, this reduced value for I_0 would also cause P to increase by about a factor of five, and this in turn would reduce the coefficient of F_d by exactly this same factor in equation (19), which would then become a satisfactory approximation.

C. Earlier Calculations

Although Radzievsky (1952) was the first to perform a thorough first order calculation for the steady-state temperature on a rotating body, Öpik (1951) seems to have anticipated an asymptotic approximation to Radzievsky's results by using only "dimensional considerations". With this method Öpik (1951) in his equation (58) estimates the "surface radiative temperature between the evening and morning points" evaluated at 1 A.U. to be (in our notation)

$$\Delta T = \frac{1}{6}\sqrt{\frac{2\pi}{\omega}} \quad \text{degrees Kelvin}$$

for a "stony sphere, with proper values for the conductivity, specific heat, and solar constant .....". The quantity under the radical sign is simply the rotation period in seconds. We can extract this same equation from our own results using equations

(7) and (13b) as follows;

$$\Delta T = 2T_0 v_1 \simeq \frac{\pi T_0}{2P} = \frac{\alpha I_0}{\sqrt{2\rho C_p K}} \quad \text{degrees Kelvin}$$

where the second step involves making an asymptotic approximation to equation (13b) for large P. Unfortunately, Öpik does not list the actual thermal parameters which he used nor does he express the functional relationship between them and ΔT. However, if we evaluate the above equation using the same thermal parameters that appeared in the numerical example above, we get simply

$$\Delta T = \frac{1}{4.9} \sqrt{\frac{2\pi}{\omega}} \quad \text{degrees Kelvin}$$

which remarkably differs by only about 20% from Öpik's estimate. Indeed, because of the wide range of thermal parameters measured in the laboratory for actual meteorites, the author feels that even now one cannot draw any firm conclusions as to which formula is more representative of the "typical" situation. The present work, however, has a more rigorous basis than Öpik's early effort.

34

IV. <u>Reradiation Forces on a Rotating Sphere</u>

Consider a sphere of radius R as shown in figure 3 which is comprised of truncated cones whose axes coincide with the sphere's spin axis which in turn is parallel to the z coordinate. If the direction of incident radiation is perpendicular to this axis, then the maximum intensity which a conical element that is tangent to the sphere at latitude θ experiences will be $I_0 \cos \theta$. If the "average" radius of such a cone is R' and its slant height measured along a conical element is L, then the normal to a differential surface element will be given by

$$dS_x = - LR'd\psi \sin \psi \cos \theta$$

$$dS_y = LR'd\psi \cos \psi \cos \theta$$

in the coordinate system of figure 1. In a manner exactly analogous to the derivation of equations (15), we find that

$$F_x(\theta) = \frac{2\alpha I_0 \cos^2 \theta}{3c(1 + \delta)} LR'U_1 \tag{20a}$$

$$F_y(\theta) = - \frac{2\alpha I_0 \cos^2 \theta}{3c(1 + \delta)} LR'V_1 \tag{20b}$$

where one factor of $\cos \theta$ comes from the fact that the reradiation pressure is always directed by the cone's slanted surface at an angle θ to the x-y plane, and the other factor of $\cos \theta$ is a consequence of the reduced incident energy on this same surface.

We must now determine how to modify the parameter P that appears in equations (11) from the cylindrical to the conical case. It has been found convenient to require that P retain its

Figure 3
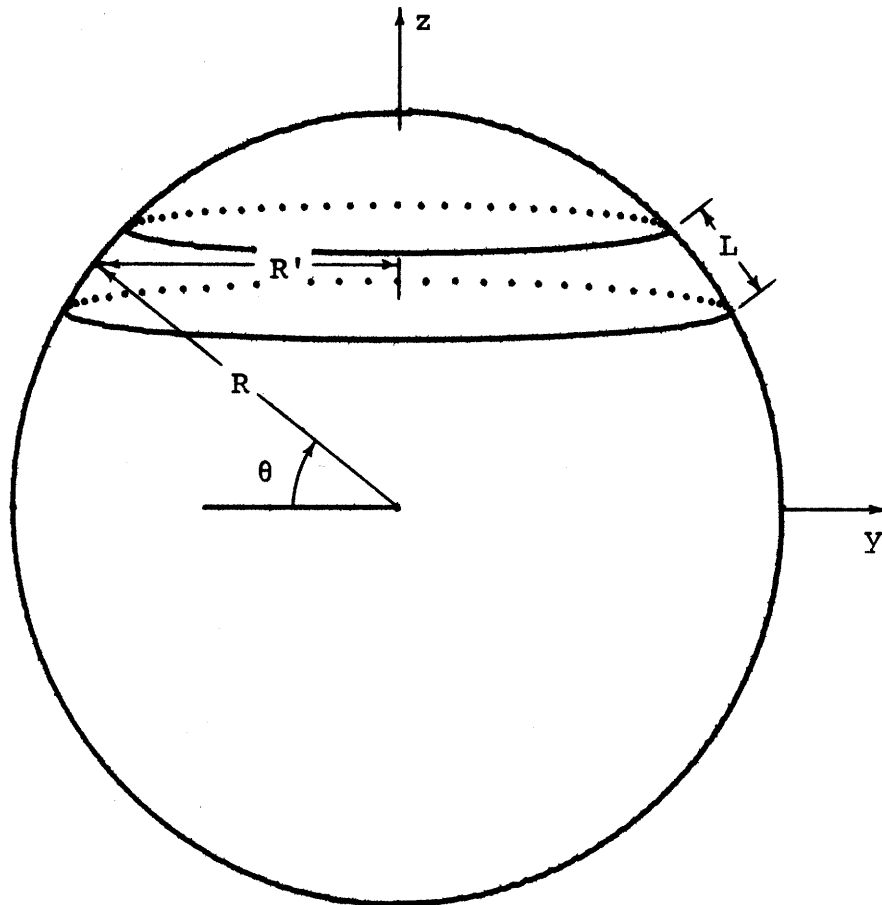
The coordinate system used for calculating the reradiation forces on an illuminated rotating sphere. Here the x coordinate is directed out of the plane of the paper, but otherwise this system is the same as that depicted in figure 1. The sphere is regarded as being comprised of many thin truncated cones with a radius of R' and a height given by $L \cos \theta = R \cos \theta \, d\theta$.

currently defined value, and then to introduce the θ dependence

of the parameter that appears in equations (11b-11g) by using

equation (11a) and the original definition of P as follows;

$$I_0(\theta) = I_0 \cos \theta \tag{21a}$$

$$T_0(\theta) = \left[\frac{\alpha I_0(\theta)}{\varepsilon \sigma \pi (1 + \delta)}\right]^{1/4} = T_0 \cos^{1/4} \theta \tag{21b}$$

$$P(\theta) = \frac{\pi T_0(\theta)}{\alpha I_0(\theta) \sqrt{2}} \sqrt{\rho C_p K \omega} = \frac{P}{\cos^{3/4} \theta} \tag{21c}$$

where the quantities I_0, T_0, and P on the right hand side of these

relationships have all had their original identities preserved.

We can now substitute equation (21c) into equations (11b) and

(11c) which can then be used to eliminate U_1 and V_1 from equation

(20) to get

$$F_x(\theta) = \frac{2\alpha I_0 \cos^2 \theta}{3c} LR' \left[\frac{\pi}{2} - \frac{P}{\cos^{3/4} \theta}(u_1 - v_1)\right] \tag{22a}$$

$$F_y(\theta) = \frac{2\alpha I_0 \cos^2 \theta}{3c} LR' \frac{P}{\cos^{3/4} \theta}(u_1 + v_1) \tag{22b}$$

in a manner exactly analogous to the derivation of equations (16).

Next we use relationship (21c) in the approximations (13) to get

the reradiative force on a rotating cone of half-angle θ as

$$F_x(\theta) = \frac{2\alpha I_0 \cos^2 \theta}{3c} LR' \pi \frac{P \cos^{3/4} \theta + 4 \cos^{3/2} \theta}{P^2 + 4P \cos^{3/4} \theta + 8 \cos^{3/2} \theta} \tag{23a}$$

$$F_y(\theta) = \frac{2\alpha I_0 \cos^2 \theta}{3c} LR' \pi \frac{P \cos^{3/4} \theta}{P^2 + 4P \cos^{3/4} \theta + 8 \cos^{3/2} \theta} \tag{23b}$$

which indeed reduce to equations (17) for a cylinder when $\theta = 0$.

In order to use these results to get the reradiation forces on a rotating sphere, first note from figure 3 that we may identify $R' = R\cos\theta$ and $L = Rd\theta$ in equations (23). Then we integrate these equations over the entire surface to get

$$F_x = \int_{-\frac{\pi}{2}}^{\frac{\pi}{2}} F_x(\theta)\,d\theta = \frac{4}{3}\,\alpha F_d \int_0^{\frac{\pi}{2}} \frac{P\cos^{15/4}\theta + 4\cos^{9/2}\theta}{P^2 + 4P\cos^{3/4}\theta + 8\cos^{3/2}\theta}\,d\theta \quad (24a)$$

$$F_y = \int_{-\frac{\pi}{2}}^{\frac{\pi}{2}} F_y(\theta)\,d\theta = \frac{4}{3}\,\alpha F_d \int_0^{\frac{\pi}{2}} \frac{P\cos^{15/4}\theta}{P^2 + 4P\cos^{3/4}\theta + 8\cos^{3/2}\theta}\,d\theta \quad (24b)$$

where the integrand's symmetry has permitted the range of integration to be halved, and F_d is again the "direct" light pressure on the sphere given by

$$F_d(\text{sphere}) = \pi R^2 I_0/c$$

which has the same physical significance as the quantity first introduced in equations (15).

The procedure used to evaluate the integrals in equations (24) is somewhat tedious, and therefore it will only be briefly sketched here. First the denonimator is factored into 2 complex products and the result is then expanded in partial fractions as follows;

$$\frac{1}{P^2 + 4P\cos^{3/4}\theta + 8\cos^{3/2}\theta} =$$

$$= \frac{i}{4P}\left(\frac{1}{\cos^{3/4}\theta + (1+i)P/4} - \frac{1}{\cos^{3/4}\theta + (1-i)P/4} \right).$$

Both terms can then be readily expanded in a power series valid for large P which permits the trigonometric terms to be integrated term by term using standard techniques. The results after some simplifications are

$$F_x = F_y + \frac{4\sqrt{\pi}}{3P} \alpha F_d \sum_{j=1}^{\infty} -\left(\frac{-\sqrt{8}}{P}\right)^j \sin\left(\frac{\pi j}{4}\right) \frac{\Gamma\left((3j+19)/8\right)}{\Gamma\left((3j+23)/8\right)} \qquad (25a)$$

$$F_y = \frac{\sqrt{\pi}}{3} \alpha F_d \sum_{j=1}^{\infty} -\left(\frac{-\sqrt{8}}{P}\right)^j \sin\left(\frac{\pi j}{4}\right) \frac{\Gamma\left((3j+16)/8\right)}{\Gamma\left((3j+20)/8\right)} \qquad (25b)$$

which can be further transformed by the method of Padé approximants on the first three terms of each series to yield the following;

$$F_x = 0.808 \frac{P + 3.79}{P^2 + 3.79\, P + 6.89} \alpha F_d \qquad (26a)$$

$$F_y = 0.808 \frac{P}{P^2 + 3.69\, P + 6.74} \alpha F_d \qquad (26b)$$

which expressions have also been constrained to take on their correct values for P = 0.

Because the basic physical processes here are the same for both cylinders and spheres, it is not surprising that equations (26) closely resemble equations (17). We would expect, however, that a sphere with its high latitude surface elements will radiate more isotropically than a cylinder and thus the resulting reradiative forces will not be as great. Due to the fact that the conditions for attaining the maximum Yarkovsky efficiency occur for a fixed value of $P/\cos^{3/4}\theta$, the higher latitude regions

of the sphere will become most efficient at a smaller value of P than for a cylinder where $\theta = 0$. Thus we would expect that the optimum value of P for the sphere as a whole will be somewhat smaller than that for the case of a cylinder. Differentiating equation (26b) with respect to P and setting the result equal to zero yields

$$P\left(F_y = \max \right) = \sqrt{6.74} \tag{27a}$$

$$\max\left(F_y \right) = 0.091 \, \alpha F_d \tag{27b}$$

which, when compared to equations (18), are seen to be exactly in accordance with our expectations as stated above.

The reader is reminded that equations (26) are derived for the case where the sphere's spin axis is perpendicular to its orbital plane. It is probably worth noticing here that equation (26b) could be amended approximately after Öpik (1951) to take into account a rotation axis inclined at an angle ι to this perpendicular by multiplying the right hand side by $\cos \iota$. With this modification retrograde rotation simply corresponds to $\iota = 180°$. Moreover, for a random distribution of spin axis orientations the average value for $\cos \iota$ will be zero while the average magnitude will be only one half of that given by equation (26b). Since many different effects are known to be capable of changing both the angular velocity and spin axis orientation of a small irregularly-shaped interplanetary fragment, a comprehensive study would be required in order to draw any useful conclusions about

40

the rotational evolution of such bodies.   Such a study is beyond
the scope of this work and so in the calculations that follow we
will simply assume a sphere with its spin axis maintained perpen-
dicular to its orbital plane.   Except for a constant factor of
cos ι, there is as yet no compelling evidence that such an assump-
tion is entirely unrealistic for fragments large enough to sur-
vive passage through the earth's atmosphere.

V. Orbital Effects from Reradiative Forces

A. Generalization of the Basic Parameters

Now that we have calculated the reradiation forces on a "large" sphere rotating about an axis which is perpendicular to the direction of incident radiation, some of the orbital changes arising from such thermal re-emissions can be determined. Because even the simplified case of orbital evolution involving gravity perturbations by Jupiter can be extremely complex, we will initially consider just the reradiative force as the only perturbation on a two-body system. Another simplification, which will be adequate to get at least some idea of the true importance of the Yarkovsky effect, can be made by replacing equations (26) with an asymptotic approximation valid for large P as follows;

$$F = F_x = F_y \simeq 0.808 \; \alpha F_d/P \tag{28}$$

which is exactly analogous to equation (19). Next, using the inverse square law of radiation intensity with distance as a basis, we determine the dependence of F on orbital distance in a manner exactly analogous to the procedure outlined in equations (21) to get

$$I_0(\mathbf{d}) = I_0/d^2 \tag{29a}$$

$$F_d(d) = \pi R^2 I_0(d)/c = \pi R^2 I_0/cd^2 \tag{29b}$$

$$T_0(d) = \left(\frac{\alpha I_0(d)}{\varepsilon \sigma \pi (1 + \delta)}\right)^{\!1/4} = T_0/\sqrt{d} \tag{29c}$$

$$P(d) = \frac{\pi T_0(d)}{\alpha I_0(d)\sqrt{2}} \; \sqrt{\rho C_p K \omega} = Pd^{3/2} \tag{29d}$$

where d is the orbital distance from the sun expressed in Astronomical Units (A.U.). When equations (29b) and (29d) are substituted into (28) we get

$$F = \frac{0.808 \; \alpha I_0 \pi R^2}{cPd^{7/2}} \tag{30}$$

where I_0 and P are now both constants to be evaluated at 1 A.U. At this point the perturbing accelerations can be readily computed by dividing both sides of equation (30) by the sphere's mass given by $m = 4\rho\pi R^3/3$ to get

$$F(d)/m = \frac{0.606 \; \alpha I_0}{cP\rho Rd^{7/2}} = Q/d^{7/2} \tag{31}$$

where $Q = \dfrac{0.606 \; \alpha I_0}{cP\rho R}$ is the reradiative acceleration on the sphere evaluated at 1 A.U.

B. Variation of Orbital Elements

Next we employ the method of the variation of orbital elements in the coordinate system of figure 1 which takes the form

$$\frac{da}{dt} = 2\sqrt{\frac{a^3}{\mu(1-e^2)}} \left(e \sin f \; \frac{F_x}{m} + (1 + e \cos f) \; \frac{F_y}{m} \right) \tag{32a}$$

$$\frac{de}{dt} = \sqrt{\frac{a(1-e^2)}{\mu}} \left(\sin f \; \frac{F_x}{m} + \frac{e + 2 \cos f + e \cos^2 f}{1 + e \cos f} \; \frac{F_y}{m} \right) \tag{32b}$$

$$\frac{d\eta}{dt} = \frac{1}{e} \sqrt{\frac{a(1-e^2)}{\mu}} \left(- \cos f \; \frac{F_x}{m} + \frac{2 + e \cos f}{1 + e \cos f} \sin f \; \frac{F_y}{m} \right) \tag{32c}$$

where a is the semimajor axis of the sphere's solar orbit, e is its eccentricity, f is the true anomaly, η is the argument of pericenter, and μ is the gravitational constant of the sun. Noting

43

that $d = a(1 - e^2)/(1 + e \cos f)$ for our two-body orbit, we substitute equation (31) into (32) and then average over a complete revolution keeping only terms in lowest nonvanishing order in e to get approximately

$$\langle \frac{da}{dt} \rangle = \pm \frac{2Q}{\sqrt{\mu} a^2} \tag{33a}$$

$$\langle \frac{de}{dt} \rangle = \pm \frac{2Qe}{\sqrt{\mu} a^3} \tag{33b}$$

$$\langle \frac{d\eta}{dt} \rangle = - \frac{3Q}{4\sqrt{\mu} a^3} \tag{33c}$$

where the notation $\langle \ \rangle$ signifies time averaging over a complete orbit. Here equations (33a) and (33b) are found to depend only upon the y component of the disturbing acceleration while equation (33c) depends only upon the x component. Thus the major changes involving the size and shape of the orbit are determined solely by the Yarkovsky force whose sign depends upon the relative sense between the sphere's spin and orbital angular velocities. In particular, if the two angular velocities have the same sense, then the plus sign in equations (33a) and (33b) is correct; otherwise the minus sign must be used. The minus sign in equation (33c) means that the orbit's pericenter will always regress. Equations (33) may be regarded as a coupled set of differential equations whose solution, which neglects the nonsecular fluctuations, is readily found to be

44

$$a(t) = a_0 \left(1 - \frac{6Q}{\sqrt{\mu a_0^3}} t \right)^{1/3} \tag{34a}$$

$$e(t) = e_0 \left(1 - \frac{6Q}{\sqrt{\mu a_0^3}} t \right)^{1/3} \tag{34b}$$

$$\eta(t) = \eta_0 + \frac{1}{8}\ln \left(1 - \frac{6Q}{\sqrt{\mu a_0^3}} t \right) \tag{34c}$$

where a_0, e_0, and η_0 are the initial values of the orbital elements at $t = 0$. Also since we are primarily interested in the case of asteroid fragments which eventually pass inside the earth's orbit, the minus sign was chosen in equations (33a) and (33b). Note that this choice corresponds to the fragment having a rotation which is retrograde with respect to its orbital motion. By comparing equations (34a) and (34b), also note that $a(t)$ and $e(t)$ maintain a ratio which is constant with time.

C. A Numerical Example

The real significance of equations (34) can best be appreciated by extending our numerical example of a previous section which illustrated the force on a rotating cylinder. Because no homogeneous set of units are particularly convenient here, we may hybridize the problem as follows. First let the quantity Q in equation (31) be evaluated in cgs units so that it has the dimensions of cm $\sec^{-2}$. If a convenient unit of time is chosen to be one million years, then we get

$$Q \; \{cm \; \sec^{-2}\} = 6.66 \times 10^{13} \; Q \; \{A.U. \; Myr^{-2}\}$$

$$\mu_{sun} = 3.956 \times 10^{13} \; A.U.^3 \; Myr^{-2}.$$

45

If we take R, the radius of our sphere, to be 50 centimeters and and require that ρ, P, and I_0 retain their previous values of 2.5 gm cm^{-3}, 17.1, and 1.4×10^6 erg cm^{-2} sec^{-1} at 1 A.U. respectively, then we get for a black stony sphere one meter in diameter

$$Q = 1.32 \times 10^{-8} \text{ cm sec}^{-2} = 8.80 \times 10^5 \text{ A.U. Myr}^{-2}$$

$$6Q/\sqrt{\mu} = 0.84 \text{ A.U.}^3 \text{ Myr}^{-1} \text{ per A.U.}^{7/2}$$

and equation (34a) becomes simply*

$$a(t) = a_0 \left(1 - 0.84 \, t/a_0^3 \right)^{1/3} \tag{35}$$

which is graphed in figure 4 for $a_0 = 3$ A.U. Note that this size sphere under the action of the Yarkovsky effect would require only about 30 million years to cross inside the earth's orbit from the middle of the asteroid belt. A larger object would take longer in proportion to its diameter, but unfortunately the situation is a bit more complex for "small" objects as we shall soon see. If the above numerical values are used in equation (34c), it is found that during the time the sphere's semimajor axis is changing from 3 A.U. to 1 A.U., its perihelion regresses only about 24^0.

As indicated by the dashed portion of the curve in figure 4, equation (35) actually breaks down in this case when the sphere gets much closer to the sun than 1 A.U. The reason for this can be seen by noticing that while equation (28) is a valid approximation to (24b) only for large values of P, equation (29d) shows

*The "extra" factor of A.U.$^{7/2}$, which appears in some of the dimensions, arises from the way in which equation (31) was derived.
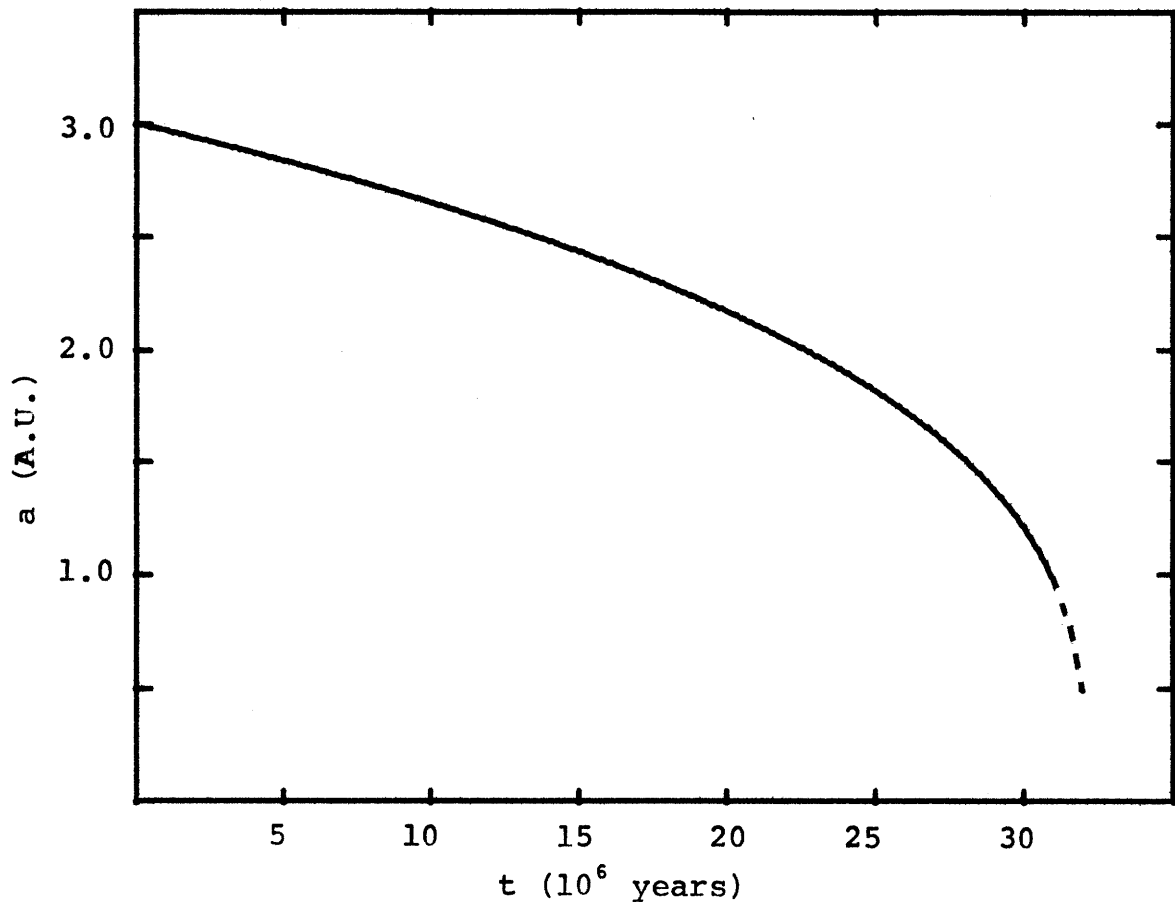
Figure 4

Possible orbit evolution of a stony meteorite one meter in
diameter under the influence of the Yarkovsky effect acting
alone. Any initial orbital eccentricity would also evolve by
following a profile identical to that shown above for the semi-
major axis. The simplifying assumptions used in obtaining equation
(30) are violated in this case when the body passes inside 1 A.U.

47

that $P(a)$ decreases with a. Therefore, the approximation (28) must breakdown ultimately as the sphere spirals into the sun. However, equations (34) are probably applicable to many cases of interest.

VI. Comparison with the Poynting-Robertson Effect

The Poynting-Robertson drag on absorbing particles in orbit about a luminous body has been well understood since its careful documentation by Robertson (1937). It arises from the fact that such a particle, while re-emitting the radiation it has absorbed, must necessarily impart net momentum to this radiation at the expense of its own orbital energy. The resulting drag on a particle which is in a circular orbit about the sun will always be in the negative y direction in our notation and can be written as

$$F_{pr} = 10^{-4} \alpha F_d / \sqrt{a} \qquad \text{(with "a" in Astronomical Units)}$$

where for a sphere again we have $F_d = \pi R^2 I_0 / c$ and where the factor of 10^{-4} comes from the ratio of the earth's orbital velocity to the speed of light. The corresponding expression for the Yarkovsky force on a sphere can be found by substituting equation (29d) into (26b) to get

$$F_y(a) = \frac{0.808 \, Pa^{3/2}}{P^2 a^3 + 3.69 \, Pa^{3/2} + 6.74} \, \alpha F_d$$

and so the ratio between the two forces is readily found to be

$$\frac{F_y}{F_{pr}} = \frac{8080 \, Pa^2}{P^2 a^3 + 3.69 \, Pa^{3/2} + 6.74} .$$

For a given value of a, this ratio is maximized when $P^2 = 6.74/a^3$, and the value attained at this maximum is then found to be $910\sqrt{a}$. These results are consistent with equations (27) which were only valid for a = 1 A.U. Although this approach demonstrates that

49

under the most favorable of circumstances the Yarkovsky force can exceed the Poynting-Robertson drag by three orders of magnitude, it also requires rather small values for P.

Perhaps a more realistic approach to the comparison of these two effects is to form the asymptotic approximation to their ratio valid for large P which is simply

$$\frac{F_y}{F_{pr}} = \frac{8080}{Pa} \qquad Pa^{3/2} > 20.$$

Here it is interesting to note that a stable balance between these forces is possible when the above ratio is unity and the sphere's spin sense is prograde with respect to its orbital motion. This fact was first pointed out by Öpik (1951). However, if P takes on a "typical" value of 20 at 1 A.U., then we may say that the Yarkovsky force is "typically" two hundred times greater than the Poynting-Robertson drag for asteroid fragments spiraling in towards the earth's orbit.

VII. The Yarkovsky Effect on "Small" Bodies

If the thermal conductivity within a rotating body is suf-
ficiently large for a given sized object, then a significant
amount of the energy absorbed at its surface can be thermally
conducted through its interior. Compared to the previously con-
sidered situation, such a process would serve to greatly diminish
the net reradiation forces on the body by reducing differences
in its surface temperature and hence, the asymmetry of emitted
thermal radiation. More quantitatively, we may say that such
internal heat conduction is important whenever $\lambda R < 4$, since this
would violate the condition used in deriving equations (5) upon
which all our analyses up to now have been based. Although this
process probably deserves as much attention as the case for
"large" bodies already considered, we will only briefly discuss
it here by following the treatment of Öpik (1951).

For the case of a "small" rotating body where $\lambda R < 4$, Öpik
(1951) derives a formula which in our notation would be approxi-
mately equivalent to

$$v_1 = - \frac{\alpha I_0 R}{17 T_0 K d^{3/2}}$$
(36)

where as before in equations (29), I_0 and T_0 are the solar flux
and equilibrium temperature respectively evaluated at 1 A.U.
Note that equation (36) displays no dependence of v_1 upon either
the heat capacity or spin rate of the body. Using equation (15b)
with $\delta = 0$, we can calculate the Yarkovsky force on a "small"

cylinder with the help of the linear approximation, $V_1 = 4v_1$, from equations (9) to get

$$F_y = -\frac{4}{3}v_1\alpha F_d.$$

If we assume that this equation is also a reasonably good approximation for a spherical body with a proper value of v_1 as given by equation (36), then we may estimate the Yarkovsky acceleration on the body at a distance d from the sun in exactly the same manner used to derive equation (31) by writing

$$\frac{F_y}{m} = \frac{\alpha^2 I_0^2}{17cKT_0\rho d^{7/2}} = \frac{Q_s}{d^{7/2}} \tag{37}$$

where as before, $Q_s = \dfrac{\alpha^2 I_0^2}{17cKT_0\rho}$ is defined as the Yarkovsky acceleration evaluated at 1 A.U. Note that the radius of the body, R, has dropped out of equation (37) which means that in this situation the y-component of acceleration is independent of size. If equation (37) were to be substituted into equations (32a) and (32b), then we would first get equations (33a) and (33b) which could then be integrated to yield equations (34a) and (34b) with Q replaced by Q_s.

The distinguishing physical parameter in equation (36) turns out to be the thermal conductivity, K. We now choose this and the other physical properties of the body to be typical of an iron-rich alloy as follows;

T = 300°K at 1 A.U. α = 0.8

K = 4 × 10^6 erg cm^{-1} °K^{-1} sec^{-1} ρ = 8.0 gm cm^{-3}

from which we compute

$$Q_s = 2.56 \times 10^{-10} \text{ cm sec}^{-2} = 1.71 \times 10^4 \text{ A.U. Myr}^{-2}.$$

When this value of Q_s is substituted into equation (34b) and the result used to compute the time necessary for the body to move from 3 A.U. to 1 A.U., we find that about 1600 Myr would be required. If we were to perform precisely the same calculation for a stony object which is "small enough" for equation (36) to apply, then we would find that only 12 Myr would be required for the body to reach 1 A.U. from an initial distance of 3 A.U. The decrease in both thermal conductivity by a factor of 25 and density by more than a factor of 3 would thus seem to indicate a rapid rate of transport for stony material from the asteroid belt by this mechanism compared to the rate for metallic material. It is interesting to note here that such a dichotomy in the rates of orbital evolution, depending upon the body's physical properties, is consistent with the cosmic ray exposure ages of meteorites as measured in the laboratory (Wasson, 1974).

It is now instructive to compare the actual sizes of stony and iron bodies for which equation (36) becomes valid. Using the criterion $\lambda R < 4$ and the respective thermal parameters as already set forth including an assumed rotation period of 5 hours, we get the condition $R < 120$ cm for the "small body" approximation to hold for an iron composition. Recall that in a previous numerical example, we showed that the corresponding condition for a stony compostion was $R < 24$ cm. Thus it would seem that the sub-

ject of reradiative effects on "small" bodies is a relevant consideration for some stony and nearly all iron meteorites.

VIII. Discussion

A. Cosmic Ray Exposure Ages

The measured cosmic ray exposure ages for stony meteorites fall in the range of 1 to 100 Myr and show a tendency to "cluster" for certain meteorite classifications (Anders, 1964;Wasson, 1974). Whether their respective parent bodies were disrupted catastrophically or gradually, the previous section showed that all "small" (R < 25 cm) retrograde-rotating stony fragments initially at 3 A.U. could be perturbed into earth crossing orbits by the Yarkovsky effect in about 12 Myr. For values of the thermal conductivity and/or bulk density which are higher than those used to obtain this figure, equation (37) shows that the exposure ages expected from this mechanism would be proportionally longer. Thus, some achondrite exposure age clusters, such as the ones at 40 Myr for aubrites and 15 - 20 Myr for diogenites, seem to be consistent with an asteroid belt origin if the Yarkovsky effect is the dominant perturbation. Moreover, this hypothesis is supported by the fact that the aubrite with the longest exposure age, Norton County, also happens to be the largest (Herzog and Anders, 1971). This is precisely what one would predict for the Yarkovsky acceleration operating on a "large" body (R > 25 cm) for which we have shown in equation (31) that, all else being equal, the expected exposure age is proportional to its radius. With this exercise in mind, the measured thermal parameters of the Norton County meteorite (Alexeyeva, 1960) were chosen for a previous numerical example in which it was calculated that this mechanism could

bring a "large" body of 50 cm radius from 3 A.U. to 1 A.U. in 30 Myr. This value, which assumes an optimum spin axis alignment and a five hour rotation period, is really quite easy to reconcile with the 100 Myr exposure age actually measured for Norton County. If this body had its spin axis tilted 60 degrees from the normal to its orbital plane and its rotation period shortened from 5 to 2 hours, then a revised theoretical calculation of the Yarkovsky effect in this instance would yield results that agreed almost exactly with the 100 Myr exposure age. Alternatively, if we retain the original spin parameters, then we can also account for the longer exposure age by simply starting at 4.4 A.U. rather than at 3 A.U. However, very few asteroids are known beyond 3.25 A.U., probably as a result of perturbations by Jupiter, and so the hypothetical spin parameters appear to be the more satisfactory quantities for adjustment in this case.

The most pronounced clustering of cosmic ray exposure ages for any meteorite group occurs at 4 Myr for H-group chondrites (Wasson, 1974). Although a single step process involving just the Yarkovsky effect on these bodies seems to be too weak by a factor of 3 to account for an asteroid belt origin at 3 A.U., it could just barely manage to account for an initial orbit at 2 A.U. A somewhat more plausible explanation may reside in a two-step mechanism which combines the Yarkovsky effect with secular and/or commensurability resonances with Jupiter. If a parent body for H-group chondrites were to lie in the asteroid belt near one of the more important resonances, then it would only be

necessary for the Yarkovsky effect to move the fragments a rela-
tively short distance until they could interact with it. Jupi-
ter's gravitational perturbations could then do the rest in a
time scale short compared to the exposure age (Williams, 1973).
Unfortunately, actual calculations on the orbital evolution of
meteorites which include these two effects combined have not yet
been done, and so on the basis of exposure age data alone the
existence of such a two-step mechanism would have to be considered
as mere speculation. However, both the Lost City and Pribram
H-group chondrites were recently found to have been in or very
near exact secular resonances with Jupiter just prior to their
atmospheric entry (Williams, 1972), and this new development adds
some measure of credence to an otherwise unsupported hypothesis.
In fact, Lost City has an exposure age of 5.5 Myr (Bogard et al,
1971) making it a member of the 4 Myr cluster.

Carbonaceous chondrites seem to have the shortest cosmic
ray exposure ages of any other meteorite class. Although there
are no obvious clusters, Wasson (1974) has observed that there
is a tendency for their exposure ages to decrease with increasing
friability. If increasing friability is correlated with both
decreasing density and thermal conductivity, then this tendency
would be consistent with what one would expect if the Yarkovsky
effect were the major perturbation on carbonaceous chondrite
orbits. However, we would have to decrease the product, ρK, for
these bodies by a factor of at least 6 in order to account for
the exposure ages of 2 to 4 Myr and still have an asteroid belt

origin. It is just possible that such conditions could be met
if these volatile rich meteorites were somehow enveloped by light
frothy material in their space environment, perhaps as a result
of out gassing within the newly created outer layers of a freshly
released fragment. Such material would completely disappear upon
atmospheric entry, and so we could never expect to actually see
a recovered carbonaceous chondrite in this condition. Alterna-
tively, as seems to be the case for some H-group chondrites, a
resonance with Jupiter might be involved, but the existence of
such a mechanism here remains to be demonstrated both theoretic-
ally and observationally.

Iron meteorites have cosmic ray exposure ages ranging from
less than 0.1 to 2.3 Gyr, which are typically 20 to 100 times
greater than the exposure ages found for stony meteorites (Wasson,
1974). It does not seem likely that this vast difference can be
adequately explained merely as a result of the greater resistance
of iron-nickel alloy to mass wastage in the solar system environ-
ment (Wasson, 1974; Wetherill, 1974). A prominent feature in the
exposure age data is a "cluster" at 650 Myr for group-III AB
irons which is usually interpreted as evidence that an iron par-
ent body somehow disrupted about 650 Myr ago, and we are still
receiving the remnants of that event. Consistent with this theory
is the fact that it has been estimated (Eberhardt and Geiss, 1964)
that the diameter of such a hypothetical body would only need to
be about 5 kilometers in order to account for the present influx
of irons reaching the earth. However, the Yarkovsky acceleration

operating upon "small" bodies could produce a similar exposure age distribution which would look almost the same whether a single parent body disrupted at one time in the past or whether a number of such bodies in the same region of the asteroid belt have been continuously producing fragments such that we are now witnessing a steady-state situation with respect to the terrestrial influx. The reason for this can again be found in equation (37) which shows that "small" bodies (i.e. those which are not large enough to maintain a substantial thermal gradient from one side to the other) will all be perturbed to the same extent by the Yarkovsky acceleration independant of size or spin rate as long as $\lambda R < 4$. Thus, from a common region within the asteroid belt, we would expect all the meteor-sized fragments to take about the same time to attain earth-crossing orbits whereupon they would survive for only a small fraction of their exposure ages (about 10 Myr) before impacting the earth or some other planet (Wetherill and Williams, 1968). Therefore, we are faced with the problem that two very different fragmentation mechanisms for a parent body in the asteroid belt could give rise to very similar exposure age distributions as sampled by the earth.

The previous section showed that pure iron bodies less than about 2 meters in diameter would require about 1.6 Gyr to reach the earth's orbit from 3 A.U. by the Yarkovsky effect. In order to account for the somewhat shorter exposure ages actually found for most irons, it is probably safe to say that resonances with Jupiter would play a very important role. The reason for this

is that the high thermal conductivity and density of irons causes their semimajor axes and other orbital elements to vary extremely slowly, thus maintaining any resonance conditions for relatively long periods of time. We have seen that the orbit of the Lost City meteorite was apparently strongly influenced by a Jovian resonance even though it only had an exposure age of 5.5 Myr. As in the case of the Yarkovsky effect, gravitational perturbations would also be independent of size and spin rate, and so the influence of such a resonance does not alter the end result of any explanation presented here concerning the clustering of cosmic ray exposure ages.

B. Earth-Based Observations of Asteroids

As a result of recent advances in determining the physical properties of asteroids, useful information concerning the surface composition of some of the brighter minor planets is now available. When high quality spectrophotometric, radiometric, and polarimetric data on asteroids are analyzed and compared to corresponding laboratory data on meteorites, diagnostic features are observed which demonstrate a compositional similarity between some asteroid surfaces and some meteoritic minerals. More specifically, the spectral reflectance curves for most asteroids tend to resemble either carbonaceous chondrites or metal-rich assemblages of metal plus silicate phases (McCord and Gaffey, 1974; Chapman, Morrison, and Zellner, 1975). However, the brightest asteroid, Vesta, is still the only one yet found with a spectral reflectance curve resembling a basaltic achondrite (eucrite).

The correlations between the spectral reflectance characteristics and orbital elements of some scores of asteroids have been reported elsewhere (Chapman, Morrison, and Zellner, 1975). It now appears that a majority of the asteroids larger than 40 km in diameter resemble carbonaceous chondrites, a comparatively uncommon class of meteorite recovered on the earth. Even allowing for the difficulty of these very friable bodies to survive earth atmospheric entry, it seems that the earth is not receiving a representative sample of asteroid belt material as we can now observe it. Actually, about 85-90% of terrestrial falls consist of ordinary chondrites, and yet from current spectral reflectance measurements the only candidates for the parent bodies of these meteorites include some very small (<10 km) Apollo and Amor class asteroids. It is hard to understand why these rather highly metamorphosed meteorites would come from such small parent bodies; they must be small (<40 km) or else we would see them; they must exist in order to account for the cosmic ray exposure ages. In brief, ground based optical observations have identified some belt asteroids as candidate parent bodies for carbonaceous chondrites, irons, stony-irons, and some types of achondrites. This thesis has shown that from a dynamical point of view, such candidates could be consistent with the cosmic ray exposure ages for most meteorites in these classes. However, these two pieces of information certainly do not serve to positively identify any particular parent body or group of parent bodies as such.

C. Effects of Jovian Resonances

Several times in this work, the role of possible secular resonances with Jupiter has been hypothesized to explain the measured cosmic ray exposure ages for some meteorites. There exist additional astronomical data which might also be accounted for by such a mechanism. If we consider either a rotating body perturbed by the Yarkovsky effect or a small particle perturbed by the Poynting-Robertson effect, then as their semimajor axes together with other orbital elements undergo continuous change, it is quite possible that nearly all such bodies will at least temporarily enter a resonance with a major planet. On the one hand Williams (1973) has shown that one major consequence of such a resonance could be a large increase in the perturbed orbit's eccentricity. On the other hand, for the case of a body spiraling in towards the sun under their influence, either the Yarkovsky or Poynting-Robertson effects by themselves would tend to decrease the orbital eccentricity (Robertson, 1937; Öpik, 1951). Because of the rather large heliocentric eccentricities (e>0.5) actually found for most Prairie Network optical meteors (McCrosky, 1967), for kilogram size objects impacting the lunar surface (Dainty, Stein, and Toksöz, 1975), for some radio meteors (Hawkins, 1962; Eshleman and Gallagher, 1962), and for most micrometeorites (Berg and Gerloff, 1970; Dohnanyi, 1972), it would seem that resonant perturbations could have a dominant influence on the orbital eccentricity of small solar system bodies. Therefore, the work on secular resonances done by Williams (1969, 1972, 1973, 1975)

62

might actually be applicable to the orbits of most meteorites and dust particles during some phases of their evolution and not be restricted to just a handful of special cases.

D. <u>Some Recommendations for Further Study</u>

A major aspect of this paper which has not yet been treated is the expected spin rates for small solar system bodies. However, in doing so one should remember that the Yarkovsky effect does not depend particularly strongly (i.e. weaker than linear dependence) on angular velocity. In calculating that surface asymmetries in non-magnetic tektites acted upon by solar light pressure could cause these bodies to suffer rotational bursting in only 60,000 years, Paddack (1969) realized that interplanetary magnetic fields would provide some spin damping to electrical conductors. Paddack (1975) has more recently concluded that for iron bodies, rotational bursting is important only for diameters smaller than about 0.01 cm. Based in part upon the relatively narrow range of asteroid rotation periods and the lack of polarization from asymmetric dust particles observed near the anti-solar point, Sparrow (1975) believes that Radzievsky (1954) and Paddack had overestimated the magnitude of such mechanisms. Actually, most meteorites do contain at least some metal, and cosmic ray exposure ages clearly show that they can remain intact in space for typically tens of millions of years. Since carbonaceous chondrites have both the shortest exposure ages for stones yet a relatively high electrical conductivity (Brecher et al, 1975), it seems that exposure ages for stones do not correlate

well with the amount of magnetic spin damping. Therefore, it appears unlikely that this destructive mechanism is important in determining the fate of most meteorites. Also observing that asteroid rotation periods fall in a fairly narrow range despite a very large dispersion in their masses, Icke (1973) has discussed various surface torques including the "ponderomotive" effect. Additional work in these areas is clearly needed, but it seems quite possible that various competing spinup and spin damping mechanisms could determine some equilibrium angular velocity for each body.

Among the various calculations presented in this thesis, there are at least three areas of analysis which should be extended. First, equation (36), which was obtained by Öpik (1951) using "dimensional considerations" for the temperature variation on a "small" body, should be explicitly rederived for a sphere. Although a previous section in this work has pretty much verified his expression for a "large" body, a calculation with a basis equally rigorous to that of equations (26) would be desirable. Second, the temperature distribution on a "large" rotating body as described by equations (13) represents a linearized approximation to a nonlinear problem, although it turns out that these equations actually yield quite satisfactory results as long as P > 5. A more complete solution which is valid for still smaller values of P would demand that the real nonlinear characteristics of this problem be fully taken into account. Such an effort would have applications for planetary science other than those

64

considered here, and this will be the subject of a future paper. Third, this work has been concerned with only two dimensional calculations both for orbital evolution and the temperature distribution on a rotating sphere. Radzievsky (1952) has considered the latter problem (linearized) in three dimensions. Three dimensional orbits were not treated here because even though the Yarkovsky acceleration may have an out-of-plane component, the forced precession of the line of nodes for a typical asteroid orbit seems rather short (about 10^5 years) for any appreciable inclination to build up. However, this effect must eventually be taken into account.

E. Conclusions

The Yarkovsky effect is powerful enough to reconcile an asteroid belt origin for many meteorites with their measured cosmic ray exposure ages. A significant property of this effect is that it operates much less efficiently on irons than on stones due to the large differences in thermal conductivity and density for these materials; correspondingly longer exposure ages are actually found for iron meteorites. From any given point in the asteroid belt, all retrograde spinning iron bodies less than about 2 meters in diameter would take about the same length of time to reach the earth's orbit under the influence of this continuous process. This means that it might not be necessary to postulate a catastrophic breakup for an iron parent body 650 million years ago in order to explain the clustering of exposure ages for group III AB iron meteorites. If one considers some possible implica-

tions of both the Yarkovsky effect and Jovian gravity perturbations operating simultaneously on a small asteroid fragment, then a two-step mechanism controlling its subsequent orbital evolution is strongly suggested. Such a mechanism could account not only for much of the cosmic ray exposure age data, but also for some of the more prominent characteristics of meteorite orbits. In particular, the existence of sufficiently powerful non-gravitational forces as outlined in this thesis eliminates for many meteorites the need to require that their parent bodies were in some special ad hoc orbit.

APPENDIX A

A. The Generalized Equations

All straightforward attempts by the author to solve equations
(11) in conjunction with definitions (9) have yielded unsatis-
factory results. Not only were the algebraic expressions pro-
duced by such efforts extremely complex, but they also generated
imaginary values for u_1 whenever $P \ll 1$. Therefore, a method has
been formulated whereby an asymptotic series for u_n and v_n valid
for large P is calculated as the **first** step. One consequence of
this treatment is that, unlike the assumption made in generating
equations (9), the order of a harmonic coefficient is now defined
by its asymptotic behavior for large P. For example, equations
(13) show that both the first and second harmonic coefficients
behave like P^{-1} asymptotically, and so we may designate u_1, v_1,
u_2, and v_2 as first order quantities. When this result is in-
corporated into equations (11f) and (11g), it is found that both
u_3 and v_3 behave like P^{-3}, and as such are third order quantities.
In fact, all odd coefficients except the first are third order
quantities while all even coefficients are first order. The
reason for this can be found in equation (3) which shows that
only the even and first harmonics are the ones directly "driven"
by the time dependent input radiation. All higher odd harmonics
are only indirectly driven by, at most, second order cross pro-
ducts comprised of first order harmonics. The foregoing argument
can be supported by displaying the general form of equations (11)

for n>1 which may be written as;

$$-\sqrt{n}P(1+\delta)(u_n - v_n) = U_n$$
$$-\sqrt{n}P(1+\delta)(u_n + v_n) = V_n + 2(1+\delta)/(n^2 - 1)$$

(A-1a)

if n is even, or

$$-\sqrt{n}P(1+\delta)(u_n - v_n) = U_n$$
$$-\sqrt{n}P(1+\delta)(u_n + v_n) = V_n$$

(A-1b)

if n is odd.

Because we originally assumed that all the Fourier coefficients in equation (7) were first order when we raised it to the fourth power, some higher order terms were inadvertently retained when we intended to keep only those of second order. However, the simplification permitted by neglecting such terms in equations (9) is more than offset by the fact that our original naive approach also neglected important second order terms from higher harmonics. If we were to expand equation (7) to include all harmonics and then carefully raise it to the fourth power while keeping all second order terms for the even harmonics and all third order terms for the odd, then we would get in place of definitions (9),

$$\delta(u_n, v_n) = 3(u_1^2 + v_1^2) + \tfrac{1}{2}S_3(0) + 6u_1 v_1 u_2 + 3v_2(v_1^2 - u_1^2)$$
$$+ \tfrac{1}{3}\sum_{n=1}^{\infty} u_{2n}\left(S_2(n) + S_4(n)\right) + \tfrac{1}{3}\sum_{n=1}^{\infty} v_{2n}\left(S_1(n) + S_3(n)\right)$$

$$U_1(u_n, v_n) = 4u_1 + 6(v_1 u_2 - u_1 v_2) + 3u_1^3 + 3u_1 v_1^2$$
$$+ u_1\left(S_3(0) - S_3(1)\right) + v_1 S_4(1)$$

68

$$V_1(u_n, v_n) = 4v_1 + 6(u_1u_2 + v_1v_2) + 3u_1^2v_1 + 3v_1^3$$
$$+ u_1S_4(1) + v_1\left(S_3(0) + S_3(1)\right)$$

$$U_2(u_n, v_n) = 4u_2 + 6u_1v_1 + S_4(1)$$

$$V_2(u_n, v_n) = 4v_2 + 3(v_1^2 - u_1^2) + S_3(1) \tag{A-2}$$

$$U_3(u_n, v_n) = 6(u_1v_2 + v_1u_2 - u_1v_4 + v_1u_4) + 4u_3 - u_1^3$$
$$+ 3u_1v_1^2 + 6v_1u_2v_2 + 3u_1(u_2^2 - v_2^2)$$
$$+ u_1\left(S_3(1) - S_3(2)\right) + v_1\left(S_4(1) + S_4(2)\right)$$

$$V_3(u_n, v_n) = 6(v_1v_2 - u_1u_2 + u_1u_4 + v_1v_4) + 4v_3 + v_1^3$$
$$- 3u_1^2v_1 + 6u_1u_2v_2 + 3v_1(v_2^2 - u_2^2)$$
$$+ u_1\left(S_4(2) - S_4(1)\right) + v_1\left(S_3(1) + S_3(2)\right)$$

where we have defined

$$S_1(n) = 3\sum_{j=1}^{n-1}\left(v_{2j}v_{2(n-j)} - u_{2j}u_{2(n-j)}\right) \qquad (n>1)$$

$$S_2(n) = 6\sum_{j=1}^{n-1} u_{2j}v_{2(n-j)} \qquad (n>1)$$

$$\tag{A-3}$$

$$S_3(n) = 6\sum_{j=1}^{\infty}\left(u_{2j}v_{2(n+j)} + v_{2j}v_{2(n+j)}\right)$$

$$S_4(n) \quad 6\sum_{j=1}^{\infty}\left(v_{2j}u_{2(n+j)} - u_{2j}v_{2(n+j)}\right)$$

Note that each of the above sums involves only products of even
harmonic coefficients, each of which is a first order factor.
Thus, the above sums are all second order quantities. We may
now generalize equations (A-2) and write an expression for all

69

the harmonic coefficients of T^4 in terms of those for T as follows;

for the $2n^{th}$ (even) harmonic with $n>1$ we have,

$$U_{2n}(u_m,v_m) = 4u_{2n} + S_2(n) + S_4(n) + O(\bar{P}^{-3})$$
$$V_{2n}(u_m,v_m) = 4v_{2n} + S_1(n) + S_3(n) + O(\bar{P}^{-3})$$

$\qquad\qquad$ (A-4a)

for the $2n+1^{st}$ odd harmonic with $n>1$ we have,

$$U_{2n+1}(u_m,v_m) = 6(u_1 v_{2n} + v_1 u_{2n} - u_1 v_{2n+2} + v_1 u_{2n+2})$$
$$+ 4u_{2n+1} + u_1\big(S_1(n) + S_3(n) - S_1(n+1) - S_3(n+1)\big)$$
$$+ v_1\big(S_2(n) + S_4(n) + S_2(n+1) + S_4(n+1)\big) + O(\bar{P}^{-4})$$

$\qquad\qquad$ (A-4b)

$$V_{2n+1}(u_m,v_m) = 6(v_1 v_{2n} - u_1 u_{2n} + u_1 u_{2n+2} + v_1 v_{2n+2})$$
$$+ 4v_{2n+1} + u_1\big(-S_2(n) - S_4(n) + S_2(n+1) + S_4(n+1)\big)$$
$$+ v_1\big(S_1(n) + S_3(n) + S_1(n+1) + S_3(n+1)\big) + O(\bar{P}^{-4})$$

where the notation $O(\bar{P}^n)$ represents a general expression for all terms of order n or smaller.

Before proceeding further into this problem, it should be stated that the derivation of equations (A-2), (A-3), (A-4), as well as many equations to follow involve extensive algebraic manipulations, most of which will not be displayed here. However, a few basic principles involved in these tedious computations can be enumerated which at least may serve to justify the form of the final results. First if we define

$$g = \sum_{n=1}^{\infty} \big(u_n \sin n\psi + v_n \cos n\psi\big)$$

then equations (7) and (8) can be written as

$$T = T_0(1 + g)$$
$$T^4 = T_0^4(1 + g)^4 \simeq T_0^4(1 + 4g + 6g^2 + \ldots\ldots)$$

$\qquad\qquad$ 70

respectively, where the second equation has only been expanded to second order for this example. Our task is to understand the form of g^2 as it relates to definitions (9). To do this we note secondly that the following identities are relevant;

$$\sin j \cos k = \left(\sin(j+k) + \sin(j-k)\right)/2 \qquad \left(u_j v_k \to U_{j+k} \text{ term}\right)$$

$$\sin j \sin k = \left(\cos(j-k) - \cos(j+k)\right)/2 \qquad \left(u_j u_k \to V_{j+k} \text{ term}\right)$$

$$\cos j \cos k = \left(\cos(j-k) + \cos(j+k)\right)/2 \qquad \left(v_j v_k \to V_{j+k} \text{ term}\right)$$

Thus a cross product term in g^2 from the jth and k^{th} harmonic of T will contribute in second order to the $(j \pm k)^{th}$ harmonic component of T^4. Now we may understand the general form for the second order contributions to U_n and V_n as follows;

$$U_n \propto \sum_{j+k=n}^{N} u_j v_k + \sum_{j-k=n}^{\infty} \pm u_j v_k$$

$$V_n \propto \sum_{j+k=n}^{N} (v_j v_k - u_j u_k) + \sum_{j-k=n}^{\infty} (v_j v_k + u_j u_k)$$

where there are only a finite number of harmonic pairs whose sum is n, but an infinite number of such pairs whose difference is n. Equations (A-3) illustrate the fruits of an exact treatment to second order.

B. A Nonlinear Asymptotic Approximation

A major computational advantage of solving for the harmonic coefficients in the form of an asymptotic series in inverse powers of P is that the higher order coefficients in such a series may be determined recursively from the lower by means of relatively simple relationships. This effectively eliminates

71

much of the complexity inherent in the nonlinear equations (A-2), (A-3), and (A-4). Let the solution series for u_n and v_n be represented by

$$u_n = \frac{u_{n,1}}{P} + \frac{u_{n,2}}{P^2} + \ldots\ldots + \frac{u_{n,m}}{P^m} + \ldots\ldots$$

$$v_n = \frac{v_{n,1}}{P} + \frac{v_{n,2}}{P^2} + \ldots\ldots + \frac{v_{n,m}}{P^m} + \ldots\ldots,$$

(A-5)

then we may simplify all of the sums in equations (A-3) to leading order by first solving for all $u_{2n,1}$ and $v_{2n,1}$. If we substitute equations (A-5) into (A-4a) and then the result into equations (A-1a), we get

$$-\sqrt{2n}P\left(\frac{u_{2n,1} - v_{2n,1}}{P}\right) = 0$$

$$-\sqrt{2n}P\left(\frac{u_{2n,1} + v_{2n,1}}{P}\right) = \frac{2}{4n^2 - 1}$$

where we have equated terms in the zeroth power of P. The solution to the above pair of equations is readily found to be

$$u_{2n,1} = v_{2n,1} = -\frac{1}{\sqrt{2n}(4n^2-1)}$$

(A-6)

for all n>0. If we likewise continue one step further and equate terms of order P^{-1}, we get

$$-\sqrt{2n}P\left(\frac{u_{2n,2} - v_{2n,2}}{P^2}\right) = \frac{4u_{2n,1}}{P}$$

$$-\sqrt{2n}P\left(\frac{u_{2n,2} + v_{2n,2}}{P^2}\right) = \frac{4v_{2n,1}}{P}$$

which may be readily solved using equation (A-6) to yield

$$u_{2n,2} = \frac{2}{n(4n^2 - 1)}$$

$$v_{2n,2} = 0 \tag{A-7}$$

for all $n > 0$. As can be seen from equation (3), the first harmonic is a special case, and it is the only first order quantity that cannot be handled by the general treatment above. Therefore, if we substitute equations (a-5) first into (A-2) and then into (11b) and (11c) and proceed in the same manner described above, we will find

$$u_{1,1} = -v_{1,1} = \pi/4$$

$$u_{1,2} = 0, \qquad v_{1,2} = \pi. \tag{A-8}$$

Because we only wish to compute the even harmonic coefficients to second order and the odd coefficients to third order, equations (A-4) show that it is only necessary to compute the sums in equations (A-3) to leading (second) order. Therefore, as a consequence of the fact that $u_{2n,1} = v_{2n,1}$ as shown in (A-6), we immediately see that $S_1(n) = S_4(n) = 0$ to leading order. This permits us in turn to simplify equations (A-4) and substitute them into (A-1) to get for $n > 1$,

$$-\sqrt{2n}P(1 + \delta)(u_{2n} - v_{2n}) = 4u_{2n} + S_2(n) + O(P^{-3})$$

$$-\sqrt{2n}P(1 + \delta)(u_{2n} + v_{2n}) = 4v_{2n} + S_3(n) \tag{A-9a}$$
$$+ 2(1 + \delta)/(4n^2 - 1) + O(P^{-3})$$

73

as the equations to be solved for the higher even harmonics, and

$$-\sqrt{2n+1}\ P(1+\delta)(u_{2n+1} - v_{2n+1}) = 6u_1(v_{2n} - v_{2n+2})$$
$$+ 6v_1(u_{2n} + u_{2n+2}) + 4u_{2n+1}$$
$$+ \frac{1}{4}\pi\left(S_3(n) - S_3(n+1) - S_2(n) - S_2(n+1)\right)P^{-1} + O(P^{-4})$$

<div align="right">(A-9b)</div>

$$-\sqrt{2n+1}\ P(1+\delta)(u_{2n+1} + v_{2n+1}) = 6u_1(-u_{2n} + u_{2n+2})$$
$$+ 6v_1(v_{2n} + v_{2n+2}) + 4v_{2n+1}$$
$$- \frac{1}{4}\pi\left(S_2(n) - S_2(n+1) + S_3(n) + S_3(n+1)\right)P^{-1} + O(P^{-4})$$

for the higher odd harmonics where we have also used the fact derived in equation (A-8) that $u_1 = -v_1 = \pi/(4P)$ to leading order. The reader is reminded that the above simplifications would not be correct if we wished to compute the even harmonics to third order or the odd harmonics to fourth order. However, because in this instance we only require the leading term for the sums defined by equations (A-3), we may use equation (A-6) to numerically evaluate the quantities $S_2(n)$ and $S_3(n)$ to second order. This has been done for $0<n<10$ and the results are displayed in table 1.

A similar simplification may be performed on equations (A-2). If this is done and the results are substituted into equations (11), we get for the first three harmonic coefficients and δ

$$\delta = 3(u_1^2 + v_1^2) + \frac{1}{2}S_3(0) + 6u_1v_1u_2 + \frac{1}{3}\sum_{n=1}^{\infty} u_{2n}S_2(n)$$
$$+ \frac{1}{3}\sum_{n=1}^{\infty} v_{2n}S_3(n)$$

74

n	$S_2(n)$	$S_3(n)$
0	0.0	0.6822338333
1	0.0	0.1000967834
2	0.3333333333	0.0359258116
3	0.0942809042	0.0176049170
4	0.0396581106	0.0101611106
5	0.0205387106	0.0064927576
6	0.0120957281	0.0044477362
7	0.0077729648	0.0032052530
8	0.0053201037	0.0024007772
9	0.0038188661	0.0018537248
10	0.0028451453	0.0014669360

Table 1

Evaluation of $S_2(n)$ and $S_3(n)$ to Leading Order

$$-P(1+\delta)(u_1-v_1) = 4u_1 + 6(v_1u_2 - u_1v_2)$$
$$+ \frac{1}{4}\pi\left(\frac{3}{8}\pi^2\bar{P}^2 + S_3(0) - S_3(1)\right)\bar{P}^1 - \pi(1+\delta)/2 + O(\bar{P}^4)$$

$$-P(1+\delta)(u_1+v_1) = 4v_1 + 6(u_1u_2 + v_1v_2)$$
$$- \frac{1}{4}\pi\left(\frac{3}{8}\pi^2\bar{P}^{-2} + S_3(0) + S_3(1)\right)\bar{P}^1 + O(\bar{P}^4)$$

$$-\sqrt{2}P(1+\delta)(u_2-v_2) = 4u_2 + 6u_1v_1 + O(\bar{P}^3)$$
$$-\sqrt{2}P(1+\delta)(u_2+v_2) = 4v_2 + S_3(1) + 2(1+\delta)/3 + O(\bar{P}^3) \tag{A-10}$$

$$-\sqrt{3}P(1+\delta)(u_3-v_3) = 6(u_1v_2 + v_1u_2 - u_1v_4 + v_1u_4)$$
$$+ 4u_3 + \frac{1}{4}\pi\left(\frac{1}{8}\pi^2\bar{P}^{-2} - 6u_2v_2 + S_2(1) - S_3(2)\right)\bar{P}^1 + O(\bar{P}^4)$$

$$-\sqrt{3}P(1+\delta)(u_3+v_3) = 6(v_1v_2 - u_1u_2 + u_1u_4 + v_1v_4)$$
$$+ 4v_3 + \frac{1}{4}\pi\left(\frac{1}{8}\pi^2\bar{P}^2 + 6u_2v_2 - S_3(1) - S_3(2)\right)\bar{P}^1 + O(\bar{P}^4)$$

The reason why these first three harmonics must be treated separately stems from the fact that the first harmonic is the only odd one which is "driven". It is thus the only first order quantity which, when cubed, can contribute to the third harmonic. It is likewise the only odd harmonic which, when squared, can contribute quadratically to the second harmonic. If we were to attempt a fourth order calculation, then it would become necessary to extend such special consideration to the fourth harmonic as well.

It is now possible to extend the collection of explicit expressions for $u_{n,m}$ and $v_{n,m}$ which began with equations (A-6) and (A-7). If we substitute these equations first into (A-5), and then the result into (A-9a) and equate terms of order $\bar{P}^{-2}$, we will get

$$u_{2n,3} = -\frac{2\sqrt{2n}}{n^2(4n^2-1)} - \frac{\sqrt{2n}}{4n}\Big[S_2(n) + S_3(n)\Big]$$

(A-11)

$$v_{2n,3} = \frac{2\sqrt{2n}}{n^2(4n^2-1)} + \frac{\sqrt{2n}}{4n}\Big[S_2(n) - S_3(n)\Big]$$

for all n>1 where, surprisingly, the second order quantity δ always manages to get itself eliminated from the equations. If we likewise substitute equations (5) together with (A-8) into (A-9a) and equate terms of order $\bar{P}^2$, we will get the leading asymptotic coefficients for the higher odd harmonics as;

$$u_{2n+1,3} = -\frac{3\sqrt{2}\,\pi}{4(2n+1)^{3/2}}\left(\frac{\sqrt{n}}{n(2n-1)} + \frac{\sqrt{n+1}}{(n+1)(2n+3)}\right)$$

(A-12)

$$v_{2n+1,3} = -\frac{3\sqrt{2}\,\pi}{4(2n+1)^{3/2}}\left(\frac{\sqrt{n}}{n(2n-1)} - \frac{\sqrt{n+1}}{(n+1)(2n+3)}\right)$$

for all n>1. Using this result and equating terms of order $\bar{P}^{-3}$, we get

$$u_{2n+1,4} = \frac{\pi}{4\sqrt{2n+1}}\Big(S_3(n+1) + S_2(n)\Big)$$

$$\frac{3\pi}{(2n+1)^{3/2}}\left[\frac{1}{n(2n-1)}\left(1 + \sqrt{2n} + \sqrt{\frac{2n}{2n+1}}\right) + \frac{\sqrt{2n+2}}{(n+1)(2n+3)}\right]$$

(A-13)

$$v_{2n+1,4} = \frac{\pi}{4\sqrt{2n+1}}\Big(S_3(n) - S_2(n+1)\Big)$$

$$+ \frac{-3\pi}{(n+1)(2n+3)(2n+1)^{3/2}}\left(1 + \sqrt{\frac{2n+2}{2n+1}}\right)$$

for all n>1.

As has already been noted, the first three harmonics must be considered separately, and those lower harmonic asymptotic coefficients which depart from the general formulas already given are as follows;

$$u_{1,3} = -\pi\left(2 + \sqrt{2}/4\right)$$

$$v_{1,3} = -\pi\left(2 - \sqrt{2}/4\right)$$

$$u_{1,4} = \pi\left(8 + \sqrt{2} + \tfrac{1}{4}S_3(1)\right)$$

$$v_{1,4} = -\pi\left(1 + \sqrt{2} + \tfrac{1}{4}S_3(0)\right) - \frac{9\pi^3}{32}$$

$$u_{2,3} = \sqrt{2}\left(\frac{3}{32}\pi^2 - \frac{2}{3} - \tfrac{1}{4}S_3(1)\right)$$

$$v_{2,3} = -\sqrt{2}\left(\frac{3}{32}\pi^2 - \frac{2}{3} + S_3(1)\right)$$

$$u_{3,4} = \pi\left(\tfrac{2}{5}\sqrt{3} + \tfrac{1}{3}\sqrt{6} + \tfrac{1}{3}\sqrt{2} + \frac{1}{12}\sqrt{3}S_3(2)\right) - \frac{1}{96}\sqrt{3}\pi^3$$

$$v_{3,4} = -\pi\left(\frac{11}{180}\sqrt{3} + \frac{1}{15} - \frac{1}{12}\sqrt{3}S_3(1)\right)$$

The above coefficients together with equations (A-6), (A-7), (A-8), (A-11), (A-12), and (A-13) have all been collected, evaluated, and tabulated through the tenth harmonic in table 2. If one desires explicit values of an harmonic coefficient when P is greater than 5 or 10, then these asymptotic formulas should be suitable for most purposes. For example, if one is interested in a particular value of u_4, then table 2 in conjunction with equation (A-5) shows that it may be calculated from the formula

$$u_4(P) = -\frac{0.033333}{P} + \frac{0.066667}{P^2} - \frac{0.158981}{P^3} \, .$$

u_n, v_n	$u_{n,1}, v_{n,1}$	$u_{n,2}, v_{n,2}$	$u_{n,3}, v_{n,3}$	$u_{n,4}, v_{n,4}$
u_1	0.785398	0.0	-7.393906	29.654240
v_1	-0.785398	3.141593	-5.172465	-16.840816
u_2	-0.235702	0.666667	0.330338	---
v_2	-0.235702	0.0	-0.401118	---
u_3	0.0	0.0	-0.731965	5.679489
v_3	0.0	0.0	-0.550585	-0.496581
u_4	-0.033333	0.066667	-0.158981	---
v_4	-0.033333	0.0	0.141019	---
u_5	0.0	0.0	-0.094830	0.768743
v_5	0.0	0.0	-0.045666	-0.104611
u_6	-0.011664	0.019048	-0.038391	---
v_6	-0.011664	0.0	0.031204	---
u_7	0.0	0.0	-0.030771	0.219423
v_7	0.0	0.0	-0.010780	-0.035794
u_8	-0.005612	0.007937	-0.014419	---
v_8	-0.005612	0.0	0.010826	---
u_9	0.0	0.0	-0.013833	0.091633
v_9	0.0	0.0	-0.003798	-0.015753
u_{10}	-0.003194	0.004040	-0.006829	---
v_{10}	-0.003194	0.0	0.004776	---

Table 2

Asymptotic Coefficients

C. Accuracy of the Linear Approximation

We will now use our nonlinear results to estimate the accuracy of the linear approximations (13a), (13b), and (17b) derived in the text for u_1, v_1, and F_y respectively. These equations may be reduced to asymptotic series valid for large P in a straightforward manner to yield

$$u_1 = \frac{\pi}{4}(P + 4)/(P^2 + 4P + 8) \simeq \frac{\pi}{4}\left(\frac{1}{P} + \frac{0}{P^2} - \frac{8}{P^3} + \ldots \right)$$

$$v_1 = -\frac{\pi}{4}P/(P^2 + 4P + 8) \simeq -\frac{\pi}{4}\left(\frac{1}{P} - \frac{4}{P^2} + \frac{8}{P^3} + \ldots \right) \tag{A-14}$$

$$F_y = \frac{\pi}{3}P\alpha F_d/(P^2 + 4P + 8) \simeq \frac{\pi}{3}\left(\frac{1}{P} - \frac{4}{P^2} + \frac{8}{P^3} + \ldots \right)F_d.$$

These may now be compared with the nonlinear results as presented in table 2 as follows;

$$u_1 = \frac{\pi/4}{P} + \frac{0}{P^2} - \frac{7.393906}{P^3} + \frac{29.654240}{P^4} + \ldots$$

$$v_1 = -\frac{\pi/4}{P} + \frac{\pi}{P^2} - \frac{5.172465}{P^3} - \frac{16.840816}{P^4} + \ldots \tag{A-15}$$

$$F_y = \frac{P}{3}(u_1 + v_1)\alpha F_d = \left(\frac{\pi/3}{P} - \frac{4\pi/3}{P^2} + \frac{4.271141}{P^3} + \ldots \right)\alpha F_d.$$

Thus we find that not only are the linear approximations correct to leading order, but they are also correct to second order for large P as well.

Next in order to investigate the accuracy for "small" P we first note that because equations (A-15) are obviously not valid for P<<1, we must restrict ourselves to P>5 where these expressions seem to converge. If the truncation errors in equations (A-15) are assumed to be less than the absolute value of the last term, we may compare these series with the rational form of equations (A-14) for P=5 and P=10 as follows;

P = 5	nonlinear series	last term	linear
u_1	0.1454	0.0475	0.1334
v_1	-0.0997	-0.0270	-0.0741
$F_y/\alpha F_d$	0.0761	0.0342	0.0988
P = 10			
u_1	0.0741	0.0030	0.0743
v_1	-0.0540	-0.0017	-0.0531
$F_y/\alpha F_d$	0.0671	0.0043	0.0708

Here it is interesting to observe that, for both values of P above, the results obtained from the linear approximation fall within the range of truncation uncertainty associated with the nonlinear expression. Thus, by comparing the nonlinear series with their contributions from the last terms, it seems likely that both approximations are within 50% of the true values for P=5 while for P=10 they are within 6.5%. As P increases, we have seen that the absolute errors of the linear approximations will

eventually all decrease as P^{-3} so that the relative errors will
fall off as P^{-2}. Thus it seems that the linear approximations will
probably be satisfactory for most purposes as long as P>10.

PART II

I. Introduction

In conducting a search for new planetary satellites, one
of the first steps an investigator undertakes is to calculate
theoretical limits on the region of space near the planet within
which stable orbital motion can take place. If valid, such a
limit, usually called a "sphere of influence", can serve to
greatly reduce the labor of such a search by excluding from it
large regions of the sky within which no satellite of the planet
could exist. The commonly used Laplace radius for the sphere
of influence about Jupiter is approximately 0.32 Astronomical
Units (A.U.). However, not long ago, using a numerical integration,
Chebotarev (1974) investigated the orbit of Palomar-Leiden Survey
object number 7617 and discovered that it was reasonable to
interpret its motion as that of a distant retrograde satellite
about Jupiter which never came closer than about 3 A.U. to that
planet. Although Chebotarev has examined the orbit of an actual
solar system object, earlier investigations into Hill's problem
by Hénon (1970) and into the distant retrograde orbits of fic-
titious Jovian satellites by Benest (1971) indicated that there
seemed to be no fundamental limit to the distance at which such
motion was stable except the sun-Jupiter distance! In each in-
stance, however, the method used by these investigators was
mostly limited to numerical integration of the basic dynamical
equations by a computer, and no analytic descriptions of these
orbits were attempted.

Given that there exists an actual solar system object which violates the Laplace criterion, it would be of interest to investigate analytically those orbits which remain entirely outside the "classical" sphere of influence. Considerable insight could thus be gained over a pure numerical approach toward a fundamental understanding of such orbits. The thrust of this part of the thesis is to describe the results of such a study.

The author's initial interest in such an investigation, however, arose from an entirely different direction - an attempt to circumvent a serious dynamical difficulty which would be encountered in the course of a close photographic mission to Mars' satellite Phobos. Since it turns out that Phobos' sphere of influence lies entirely within its own solid surface, it would be impossible to place a spacecraft (third body) in a Keplerian orbit about that satellite (secondary). Unfortunately, the same gravity field of Phobos, which is too weak to hold onto satellites of its own, also turns out to be too strong for a spacecraft to long remain in a Mars orbit that either closely leads or closely follows Phobos. In order to illustrate the origin of this latter difficulty, consider a spacecraft which is in the same circular orbit about Mars as Phobos, but which starts out a little behind it. Initially the spacecraft will be "stationkeeping" with Phobos and there will be no relative velocity between them. But in this configuration the small gravitational attraction of Phobos will soon succeed in "accelerating" the spacecraft into a higher orbit. Since Mars would

still be exerting the dominant gravitational force on both bodies, this higher orbit will cause the spacecraft to fall behind Phobos, and the distance between the two will then continuously increase. By a similar argument, if we start with the spacecraft slightly ahead, then the continuous retarding force of that satellite on the spacecraft will lower its orbit causing it then to continuously gain distance on Phobos. Thus we have the apparent paradox that attractive forces between two small masses, each in orbit about a massive primary, act to effectively repel each from the other! This same result is more elegantly illustrated by the well known result of the restricted three-body problem in which only two libration points, each a full orbital radius away from the secondary, are shown to be stable.

II. The Variation Orbit

The type of orbit investigated by the author in an attempt to overcome the difficulties mentioned above is illustrated in its simplest form in figure 1. We assume we have a small secondary of mass M in a circular orbit about a primary whose gravitational constant (GM$_p$) is μ. If the semimajor axis of the secondary's orbit is a, then its mean motion, n, is given by n = $\sqrt{\mu/a^3}$. Our coordinate system is centered on, and rotates with, the secondary at an angular velocity n. We identify +x as the outward radial coordinate and +y as the direction of the secondary's motion. This same coordinate system was used by Hill in his three-body study of the Moon's orbit about the Earth, and the dynamical equations he derived are

$$\frac{d^2x}{dt^2} = 2n \frac{dy}{dt} + 3n^2x - \frac{GMx}{r^3}$$

$$\frac{d^2y}{dt^2} = -2n \frac{dx}{dt} - \frac{GMy}{r^3} \qquad \text{where} \quad r = \sqrt{x^2+y^2}.$$

(1)

If at first we neglect the secondary's mass and only look for <u>periodic</u> solutions to equations (1), we get

$$x = -d_0 \cos nt$$

$$y = 2d_0 \sin nt + \text{constant} \qquad \text{(for some fixed } d_0\text{)}$$

(2)

which precisely describes the variation orbit shown in figure 1 when the arbitrary constant is zero. The initial conditions are deliberately chosen so that at t = 0 the (massless) third body is

VARIATION ORBIT ABOUT A SMALL SECONDARY

Primary

Primary – secondary line rotates at n, the seconary's (constant) angular velocity.

If f is the true anomaly of the secondary's orbit, then we have $\boxed{f = nt.}$

Path of third body as seen by the secondary.

A_y

d_0

β

d

A_x

d_0

Secondary

y

x

The variation orbit is described as follows:

$$\boxed{\begin{aligned} x &= -d_0 \cos nt \\ y &= 2d_0 \sin nt \end{aligned}}$$

Identity:

$$\tan \beta = -\frac{y}{x} = \frac{2d_0 \sin nt}{d_0 \cos nt}$$

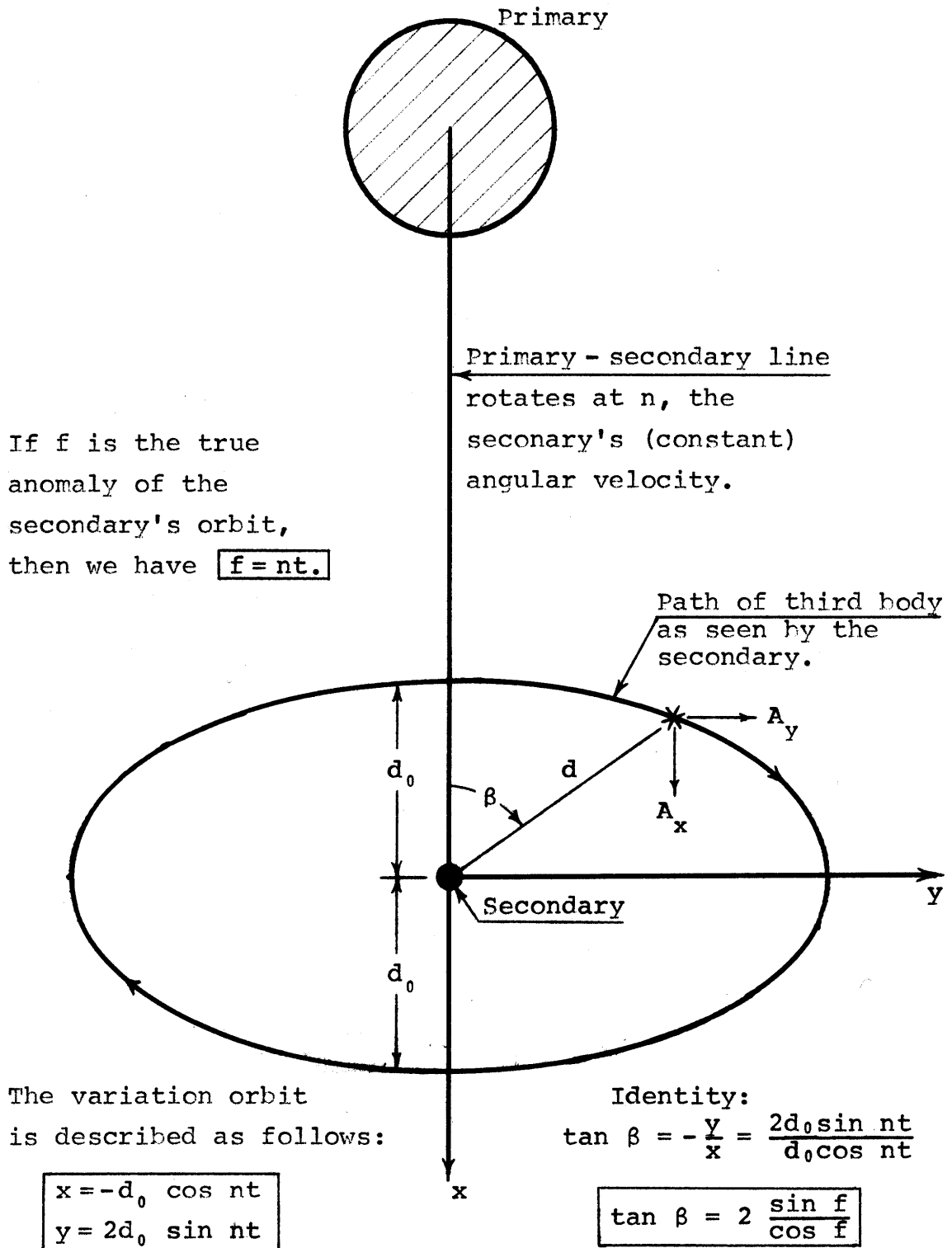$$\boxed{\tan \beta = 2\,\frac{\sin f}{\cos f}}$$

Figure 1

closest to the primary. The reason for this, illustrated in fig-
ure 2, is that the third body is in a Keplerian orbit about the
primary and orbital angles are customarily measured from peri-
center. This figure also shows that while these retrograde
variation orbits appear to encircle the secondary in our rotating
(posigrade) reference frame, the mean direction of a line joining
the $\overset{\text{second and third}}{\wedge}$ bodies would remain nearly constant in a non-rotating
frame. Also note from equations (2) that for any d_0, the varia-
tion orbit's period about the secondary is constrained to be the
same as that of the secondary's period about the primary since
both motions proceed at an angular frequency of n. Further note
that the shape and orientation of the elliptical variation orbit
is also independent of d_0.

Another result that we will need later is the "stationary
solution" found by setting $\ddot{x} = \ddot{y} = \dot{x} = \dot{y} = 0$ in equations (1). If
the secondary's mass is not neglected, then we get two algebraic
equations whose solution is

$$r^3 = \pm x_\ell^3 = \frac{GM}{3n^2}$$

(3)

$$y = 0.$$

This means that there exists two stationary points equidistant
from the secondary along the x axis at the so-called "libration"
distance which we have defined as x_ℓ. This result corresponds
to two of the well known Lagrangian librations points, L_1 and L_2,
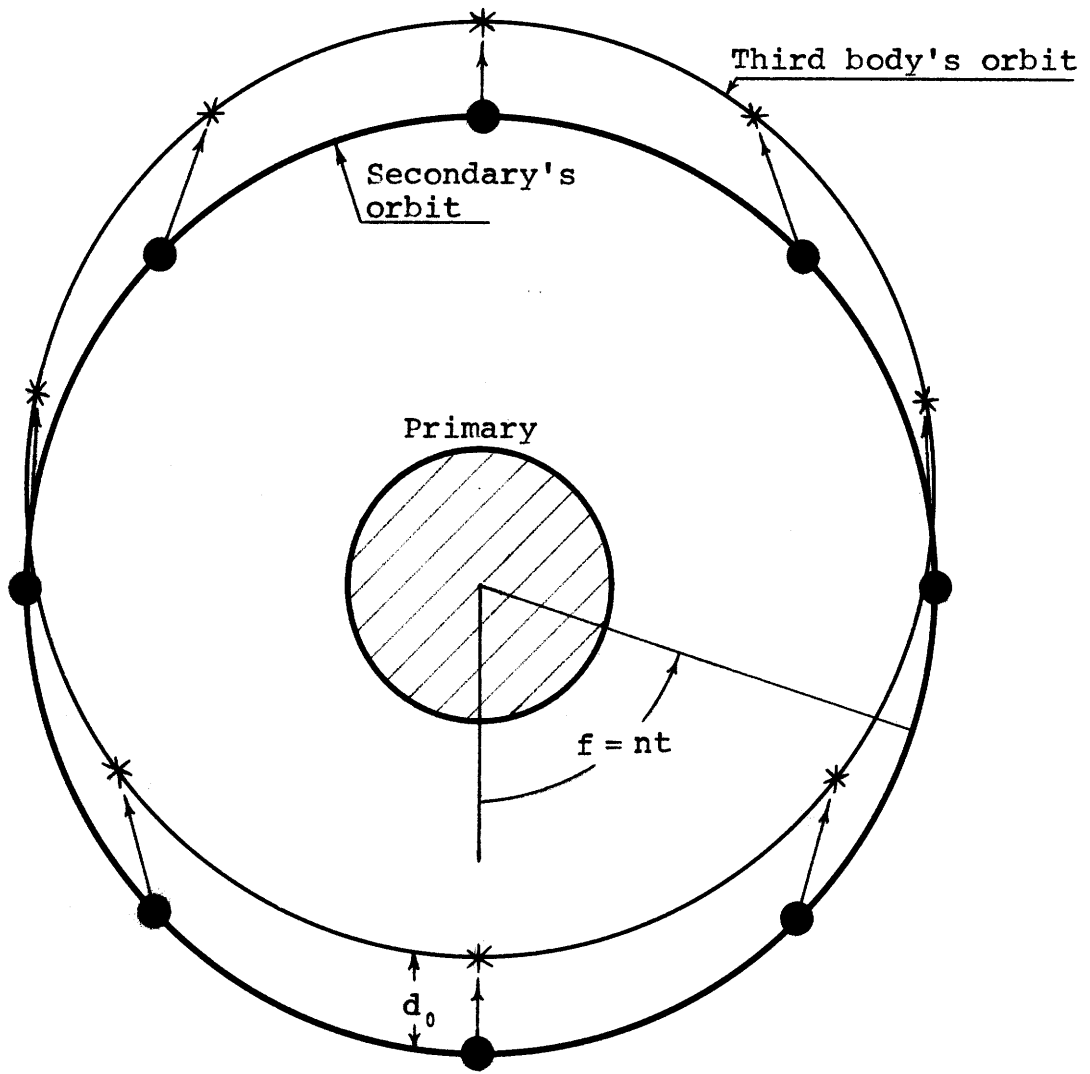of the restricted three-body problem.

Figure 2

Variation orbit in an inertial coordinate system
(neglecting the gravitational perturbation of the secondary)

III.   The Perturbed Variation Orbit

A.   Disturbing Accelerations

Now that we have established the existence of a variation orbit about a massless secondary, let us consider the effect of its (small) gravitational perturbation on the third body.   Let d be the (changing) distance between the two bodies, and let β be the angle as shown in figure 1.   If we define A_x and A_y as the radial and tangential components, respectively, of this perturbing acceleration, then we have

$$A_x = \frac{GM}{d^2} \cos \beta \qquad A_y = -\frac{GM}{d^2} \sin \beta$$

where G is the universal gravitation constant.   Since the secondary is in a circular orbit, the angle f is a linear function of time (i.e. $f = nt$).   Our task then is to find A_x and A_y as functions of f.

If we pursue the special case where the secondary is exactly in the center of the elliptical variation orbit, we can see from figure 1 and equations (2) that

$$d = \sqrt{x^2+y^2} = d_0\sqrt{\cos^2 f + 4 \sin^2 f} = d_0\sqrt{\frac{5}{2}\left(1 - \frac{3}{5}\cos 2f\right)}. \qquad (4)$$

Since it is also identically true from figure 1 that $\tan \beta = -x/y$, we have

$$\frac{\sin^2\beta}{\cos^2\beta} = \tan^2\beta = \left(\frac{y}{x}\right)^2 = 4 \tan^2 f$$

from which there follows

$$\sin \beta = \frac{2 \tan f}{\sqrt{1 + 4 \tan^2 f}} = \frac{2 \sin f}{\sqrt{\frac{5}{2}\left(1 - \frac{3}{5}\cos 2f\right)}}$$ (5)

$$\cos \beta = \frac{1}{\sqrt{1 + 4 \tan^2 f}} = \frac{\cos f}{\sqrt{\frac{5}{2}\left(1 - \frac{3}{5}\cos 2f\right)}}$$

In order to examine the stability of the retrograde variation orbit, it is also necessary to consider the situation when the secondary is not at its exact center. The geometry illustrating this case is shown in figure 3 where the x and y offsets of the center from the secondary are denoted by $\tilde{x}$ and $\tilde{y}$, respectively. It should be noted that the quantities d and β in figure 3 are still the same as those just calculated in equations (4) and (5). However, our previous expressions for A_x and A_y must be amended to read

$$A_x = \frac{GM}{r^2} \sin \delta \qquad A_y = -\frac{GM}{r^2} \cos \delta$$ (6)

where now r is the distance between the second and third bodies. The projections of r onto the x and y axes are readily seen from figure 3 to be

$$r_x = d \cos \beta - \tilde{x} \qquad r_y = d \sin \beta + \tilde{y}$$
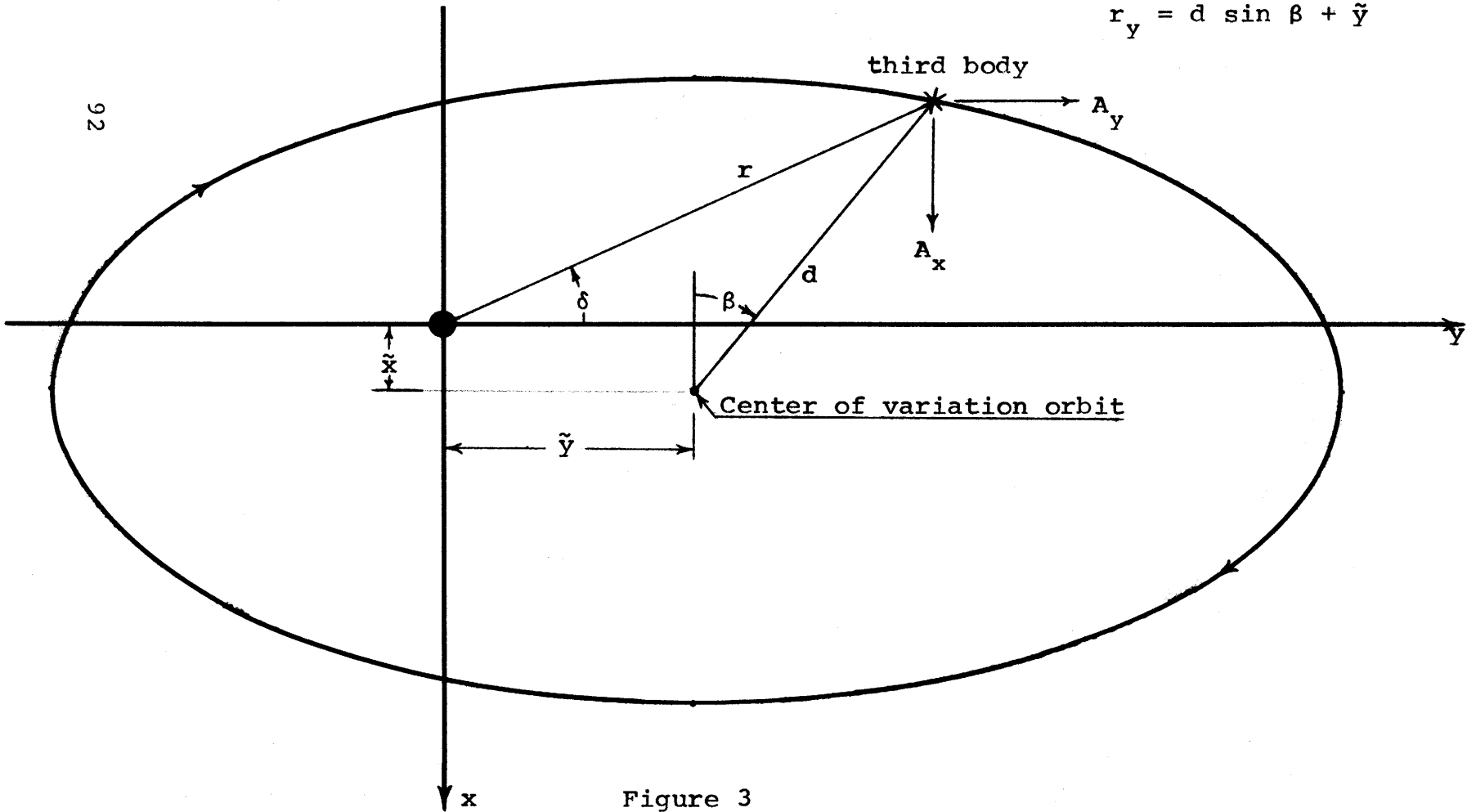
from which we immediately get

$$\sin \delta = \frac{r_x}{r} = \frac{d \cos \beta - \tilde{x}}{r} , \qquad \cos \delta = \frac{r_y}{r} = \frac{d \sin \beta + \tilde{y}}{r}$$ (7)

$$r^2 = r_x^2 + r_y^2 = d^2 + 2d\tilde{y} \sin \beta - 2d\tilde{x} \cos \beta + \tilde{x}^2 + \tilde{y}^2$$

91

Perturbations on an off-center Variation Orbit

$$r_x = d \cos \beta - \tilde{x}$$

$$r_y = d \sin \beta + \tilde{y}$$

Figure 3

Using these results to evaluate equations (6) we get

$$A_x = \frac{GM}{r^3} (d \cos \beta - \tilde{x}) \quad , \quad A_y = -\frac{GM}{r^3} (d \sin \beta + \tilde{y}) \tag{8}$$

At this point the complicated form for r^3 in the denominator of equations (8) can benefit from the approximation that both $\tilde{x}$ and $\tilde{y}$ remain small compared to d. Thus, raising both sides of equation (7) to the -3/2 power we get

$$\frac{1}{r^3} = \frac{1}{d^3} \left(1 + 2\frac{\tilde{y}}{d} \sin \beta - 2\frac{\tilde{x}}{d} \cos \beta + \frac{\tilde{x}^2}{d^2} + \frac{\tilde{y}^2}{d^2} \right)^{-3/2}$$

$$\simeq \frac{1}{d^3} \left(1 - 3\frac{\tilde{y}}{d} \sin \beta + 3\frac{\tilde{x}}{d} \cos \beta \right) \tag{9}$$

where we have neglected quadratic terms in $\tilde{x}$ and $\tilde{y}$, and then applied the binomial theorem to the remaining terms as $(1 + \alpha)^\gamma \simeq 1 + \alpha\gamma$. Another simplification we have made, which might not be obvious, is to assume that d_0 is constant, an assumption that will be justified later on. Substituting the results of equation (9) into (8) and again neglecting second order terms we get

$$A_x \simeq GM \left(\frac{\cos \beta}{d^2} + \left(\frac{3 \cos^2 \beta - 1}{d^3} \right) \tilde{x} - \left(\frac{3 \sin \beta \cos \beta}{d^3} \right) \tilde{y} \right)$$

$$A_y \simeq -GM \left(\frac{\sin \beta}{d^2} + \left(\frac{3 \sin \beta \cos \beta}{d^3} \right) \tilde{x} - \left(\frac{1 - 3 \sin^2 \beta}{d^3} \right) \tilde{y} \right) \tag{10}$$

This result when combined with equations (4) and (5) will yield A_x and A_y explicitly as functions of f and hence of time.

B. Variation of Orbital Elements

Our next task is to find what effects these perturbations will have on the third body's variation orbit about the secondary. We will consider secular changes in the variation orbit's center ($\tilde{x}$ and $\tilde{y}$), in its size (d_0), and in its frequency of motion (n). In a non-rotating reference frame, changes in d_0 correspond to variations in the eccentricity ($e = d_0/a$) of the third body's orbit about the primary, and changes in $\tilde{x}$ correspond to variations in the semimajor axis, a. Also, if a is constant, then small changes in n for the variation orbit described by equations (2) correspond to the line of apsides of the third body's Keplerian orbit about the primary undergoing a constant rotation ($\frac{d\omega}{dt}$) in inertial space as shown in figure 4. Quantitatively, we can make use of the well known variation of parameters formulae which for a nearly circular orbit reduce to

$$\frac{d\omega}{dt} = -\sqrt{\frac{a}{\mu}} \frac{1}{e} \left(\cos f \, A_x - 2 \sin f \, A_y \right) \tag{11}$$

$$\frac{da}{dt} = 2 \sqrt{\frac{a^3}{\mu}} \, A_y \tag{12}$$

$$\frac{de}{dt} = \sqrt{\frac{a}{\mu}} \left(\sin f \, A_x + 2 \cos f \, A_y + e A_y \right). \tag{13}$$

(Normally, we would have to use a bit more care than this in simplifying these equations, but it will soon be clear why, in this case, we may dispense with such complications.) Since $e = d_0/a$, we may expand the left hand side of (13) as

94
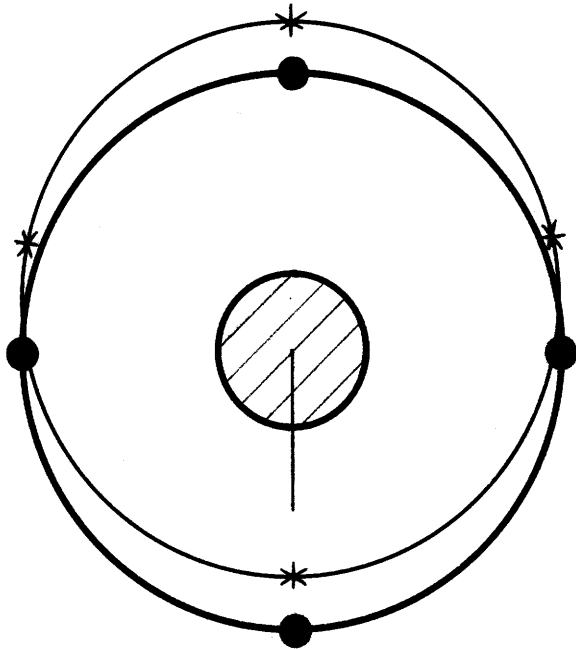
Configuration
at t = t_0

The regression of the line
of apsides in a non-rotating
coordinate system.
(Includes the gravitational
perturbation of the secondary
on the third body.)
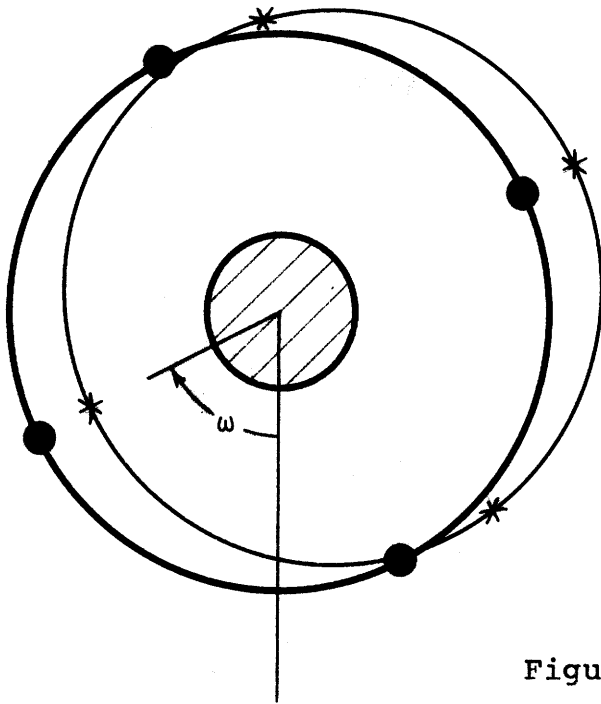
Configuration
at t > t_0

Figure 4

$$\frac{de}{dt} = \frac{d}{dt}\left(\frac{d_0}{a}\right) = \frac{1}{a}\frac{d}{dt}(d_0) - \frac{d_0}{a^2}\frac{da}{dt} \ .$$

Substituting this into equation (13) and using (12) to eliminate the $\frac{da}{dt}$ term we finally get

$$\frac{d}{dt}(d_0) = \sqrt{\frac{a^3}{\mu}}\left(\ \sin f\ A_x + 2\cos f\ A_y + 3\frac{d_0}{a}A_y\right). \qquad (14)$$

Although we now have expressions for the instantaneous rates of variation for ω, a, and d_0, we are really interested in the secular changes in these quantities ever many orbital cycles (assuming, of course, that only small changes accrue during one cycle). If we now proceed to average equations (11), (12), and (14) over one cycle, then the only additional change in any left hand member is that we may identify $\frac{da}{dt}$ as synonomous with $\frac{d\tilde{x}}{dt}$. If we similarly average the right hand members of these equations, it is necessary to compute $<A_y>$, $<A_x \sin f>$, $<A_x \cos f>$, $<A_y \sin f>$, and $<A_y \cos f>$. Explicitly, this is done by substituting equations (4) and (5) into equation (10), forming the above expressions, and then averaging for $0 < f < 2\pi$. This messy operation is displayed in table 1 where in order to conserve space, we have defined $D = \sqrt{(5/2)(1-(3/5)\cos 2f)}$. The result of numerically carrying out the integrals indicated in table 1 is as follows;

$$<A_y> = -(0.385491 - 0.485808)GM\tilde{y}/d_0^3 = 0.100317\ GM\tilde{y}/d_0^3$$

$$<A_x \cos f> = 0.285175\ GM/d_0^2$$

$$<A_y \sin f> = -0.200633\ GM/d_0^2$$

$$<A_x \sin f> = <A_y \cos f> = 0\ .$$

$$\sqrt{\frac{5}{2}\left(1 - \frac{3}{5}\cos 2f\right)}$$

$$\frac{2\ \sin f\ df}{D^3} + \frac{\tilde{x}}{d_0^3}\int_0^{2\pi} \frac{6\ \sin f\ \cos f\ df}{D^5} + \boxed{\frac{\tilde{y}}{d_0^3}\left(\int_0^{2\pi} \frac{df}{D^3} - \int_0^{2\pi} \frac{12\ \sin^2 f\ df}{D^5}\right)}$$

$$\int_0^{2\pi} \frac{\sin f\ \cos f\ df}{D^3} + \frac{\tilde{x}}{d_0^3}\left(\int_0^{2\pi} \frac{3\ \sin f\ \cos^2 f\ df}{D^5} - \int_0^{2\pi} \frac{\sin f\ df}{D^3}\right) - \frac{\tilde{y}}{d_0^3}\int_0^{2\pi} \frac{6\ \sin^2 f\ \cos f\ d}{D^5}$$

$$\int_0^{2\pi} \frac{\cos^2 f\ df}{D^3} + \frac{\tilde{x}}{d_0^3}\left(\int_0^{2\pi} \frac{3\ \cos^3 f\ df}{D^5} - \int_0^{2\pi} \frac{\cos f\ df}{D^3}\right) - \frac{\tilde{y}}{d_0^3}\int_0^{2\pi} \frac{6\ \sin f\ \cos^2 f\ df}{D^5}$$

$$\int_0^{2\pi} \frac{2\ \sin^2 f\ df}{D^3} + \frac{\tilde{x}}{d_0^3}\int_0^{2\pi} \frac{6\ \sin^2 f\ \cos f\ df}{D^5} + \frac{\tilde{y}}{d_0^3}\left(\int_0^{2\pi} \frac{\sin f\ df}{D^3} - \int_0^{2\pi} \frac{12\ \sin^3 f\ df}{D^5}\right)$$

$$\int_0^{2\pi} \frac{2\ \sin f\ \cos f\ df}{D^3} + \frac{\tilde{x}}{d_0^3}\int_0^{2\pi} \frac{6\ \sin f\ \cos^2 f\ df}{D^5} + \frac{\tilde{y}}{d_0^3}\left(\int_0^{2\pi} \frac{\cos f\ df}{D^3} - \int_0^{2\pi} \frac{12\ \sin^2 f\ \cos f}{D^5}\right.$$

Table 1

This enormous simplification is a result of 16 out of the 20 integrals in table 1 vanishing identically. This is why we could afford to be a bit hasty in simplifying the variations of parameters formulae (11) - (13); the coefficients of many of their small terms turn out to be zero.

If we now utilize these results in equations (11), (12), and (14), we get

$$\frac{d\omega}{dt} = -0.68644 \frac{GM}{nd_0^3} = -2.05932 \ n\left(\frac{x_\ell}{d_0}\right)^3 \tag{15}$$

$$\frac{d\tilde{x}}{dt} = 0.20063 \frac{GM}{nd_0^3} \tilde{y} = 0.60189 \ n\left(\frac{x_\ell}{d_0}\right)^3 \tilde{y} \tag{16}$$

$$\frac{d}{dt}(d_0) = 0.30095 \frac{GM}{and_0^2} \tilde{y} = 0.90285 \ n\left(\frac{x_\ell^3}{d_0^2 a}\right)\tilde{y} \tag{17}$$

where we have used equation (3) to eliminate the quantity GM. Also as before $n = \sqrt{\mu/a^3}$ and we have used the fact that $e = d_0/a$. If we had allowed d_0 to vary explicitly beginning with equation (9), the only contribution would have been to add an extra term to $\frac{d\omega}{dt}$ in equation (15). But we will soon see from equation (17) that this was in fact unnecessary for examining the stability of the system to first order.

C. Analytic Approximation to the Perturbed Variation Orbit

Equations (15), (16), and (17) represent three equations in the four unknowns $\tilde{x}$, $\tilde{y}$, ω, and d_0. In order to obtain a fourth equation recall that for Hill's equations (1), only periodic solutions are represented by equations (2) for a negligible

mass, M. If we search for a (independent) <u>secular</u> solution to (1) with $M = 0$ by setting $\ddot{x} = \ddot{y} = 0$, we get

$$\dot{y} = -\frac{3}{2}nx \qquad \dot{x} = 0.$$

Since this represents a constant y "drift" corresponding to any steady x displacement, the same will be true of their average values if x and y oscillate rapidly. Thus we are justified in identifying such average values with $\tilde{x}$ and $\tilde{y}$ because the center of the variation orbit is certainly an "average" of sorts for the motion around it. Our fourth equation then is

$$\frac{d\tilde{y}}{dt} = -\frac{3}{2}n\tilde{x}. \tag{18}$$

In solving the system of equations (15) – (18) first note that (16) and (18) represent two equations in the two unknowns $\tilde{x}$ and $\tilde{y}$. Differentiating (16) and using the result to eliminate $\frac{d\tilde{y}}{dt}$ from (18) we get (assuming for now that $d_0 =$ constant)

$$\frac{d^2\tilde{x}}{dt^2} + 0.90285\ n^2 \left(\frac{x_\ell}{d_0}\right)^3 \tilde{x} = 0.$$

This is just an elementary differential equation for a harmonic oscillator, so arbitrarily setting $\tilde{x}(t=0) = 0$ we get

$$\tilde{x}(t) = \tilde{x}_0 \sin \psi t \tag{19}$$

where $\tilde{x}_0$ is a constant and ψ, the libration frequency of the center of the variation orbit about the secondary, is given by

$$\psi = 0.9502\ n\left(\frac{x_\ell}{d_0}\right)^{3/2}. \tag{20}$$

We may now calculate $\tilde{y}(t)$ by substituting equation (19) into (16) and making use of equation (20) to get

$$\tilde{y}(t) = \frac{3n}{2\psi^2} \frac{d\tilde{x}}{dt} = \underbrace{\frac{3}{2} \frac{n}{\psi} \tilde{x}_0}_{\equiv \tilde{y}_0} \cos \psi t \tag{21}$$

where we have identified, by inspection, the quantity $\frac{3}{2}n\tilde{x}_0/\psi$ with the amplitude of the $\tilde{y}$ excursion which we define as $\tilde{y}_0$. The ratio of the maximum $\tilde{y}$ excursion to the maximum $\tilde{x}$ excursion then is just

$$\frac{\tilde{y}_0}{\tilde{x}_0} = \frac{3}{2} \frac{n}{\psi} = 1.5786 \left(\frac{d_0}{x_\ell}\right)^{3/2} \tag{22}$$

which thus turns out to be independent of n. Equations (19) and (21) taken together show that the center of the variation orbit itself librates about the secondary in a retrograde sense. This motion proceeds at an angular velocity of ψ as given by equation (20). Furthermore, the axes of this libration orbit are not fixed in a two-to-one ratio as is the case with the variation orbit, but the libration orbit becomes increasingly elongated in the y direction as d_0 increases.

If we rewrite equation (17) using equation (20) we get

$$\frac{d}{dt}(d_0) = \frac{d_0}{an} \psi^2 \tilde{y}$$

If we likewise rewrite equation (16) and solve for $\tilde{y}$ we get

$$\tilde{y} = \frac{3}{2} \frac{n}{\psi^2} \frac{d\tilde{x}}{dt}$$

and eliminating $\tilde{y}$ from both of the above equations yields

$$\frac{d}{dt}(d_0) = \frac{3}{2} \frac{d_0}{a} \frac{d\tilde{x}}{dt}$$

If we now divide through by d_0 and integrate both sides, we finally get

$$d_0(t) = d_0(0) \exp\left(\frac{3\tilde{x}(t)}{2a}\right) \simeq d_0(0)\left(1 + \frac{3}{2a}\tilde{x}(t)\right) \tag{23}$$

which approximation should remain valid since $\frac{\tilde{x}_0}{a} <<< 1$ and $\tilde{x}(t)$

does not grow with time. From this analysis one can conclude

that to first order in d_0/a, the variation orbit is stable against

a small $\tilde{x}$ or $\tilde{y}$ displacement of its center.

Finally, observe from figure 4 that if counterclockwise

motion is taken as positive, we may use equation (15) to get the

perturbed angular velocity, n', of the variation orbit in the form

$$n' = n - \frac{d\omega}{dt} = n\left(1 + 2.0593\left(\frac{x_\ell}{d_0}\right)^3\right) \tag{24}$$

To see this, imagine that the orbital motion of both bodies

about the primary (at the rate n) is suddenly frozen. If we do

this at $t = 0$ and then allow ω to become increasingly negative

while invoking the x vs y constraint of the variation orbit, it

can be seen that the third body then must move clockwise about

the secondary in direct measure to $-\omega$. Since this clockwise

(retrograde) motion of the variation orbit corresponds to the

normally positive n in equation (2) as both secondary and third

101

body normally orbit the primary counterclockwise, a negative $\frac{d\omega}{dt}$ increases the variation orbit's angular frequency (n').

IV. Comparison of the Analytic Results with a Numerical Integration

In order to test the accuracy of the various approximations made in the previous sections as well as to gain some appreciation of the stability of distant retrograde orbits, computer simulations of Hill's equations were made for such orbits about Jupiter. Using a 500 hour time step, a fourth order Runge-Kutta proceedure for this task was implemented on a Hewlett-Packard 9820A programmable desk calculator. For purposes of checking the numerical accuracy, the Jacobi constant for Hill's problem was formed and tracked throughout the integration; it remained constant to better than one part in 10^7.

The first case investigated numerically, which is plotted in figure 5, was that of a fictitious asteroid with $d_0 = 1.06$ A.U. and the moderately large libration amplitude of $\tilde{y}_0 = 0.65 \, d_0$. The second case more nearly resembled the orbit of Palomar-Leiden object 7617 with $d_0 = 3.02$ A.U. and $\tilde{y}_0 = 0.66 \, d_0$. The first two columns of table 2 display the parameters of the orbits generated by these numerical investigations together with the analytically determined parameters predicted by equations (20), (22), and (24). (Here $x_\ell = 0.355$ A.U. for the sun-Jupiter system.) It is thus seen that our analytic methods yield results which differ by no more than 5.1% from the exact values. The actual orbit of Palomar-Leiden object 7617 has $\tilde{y}_0 > d_0$, but this case was not investigated because the linear approximations used to obtain equations (10) break down for such a large libration amplitude. However, such
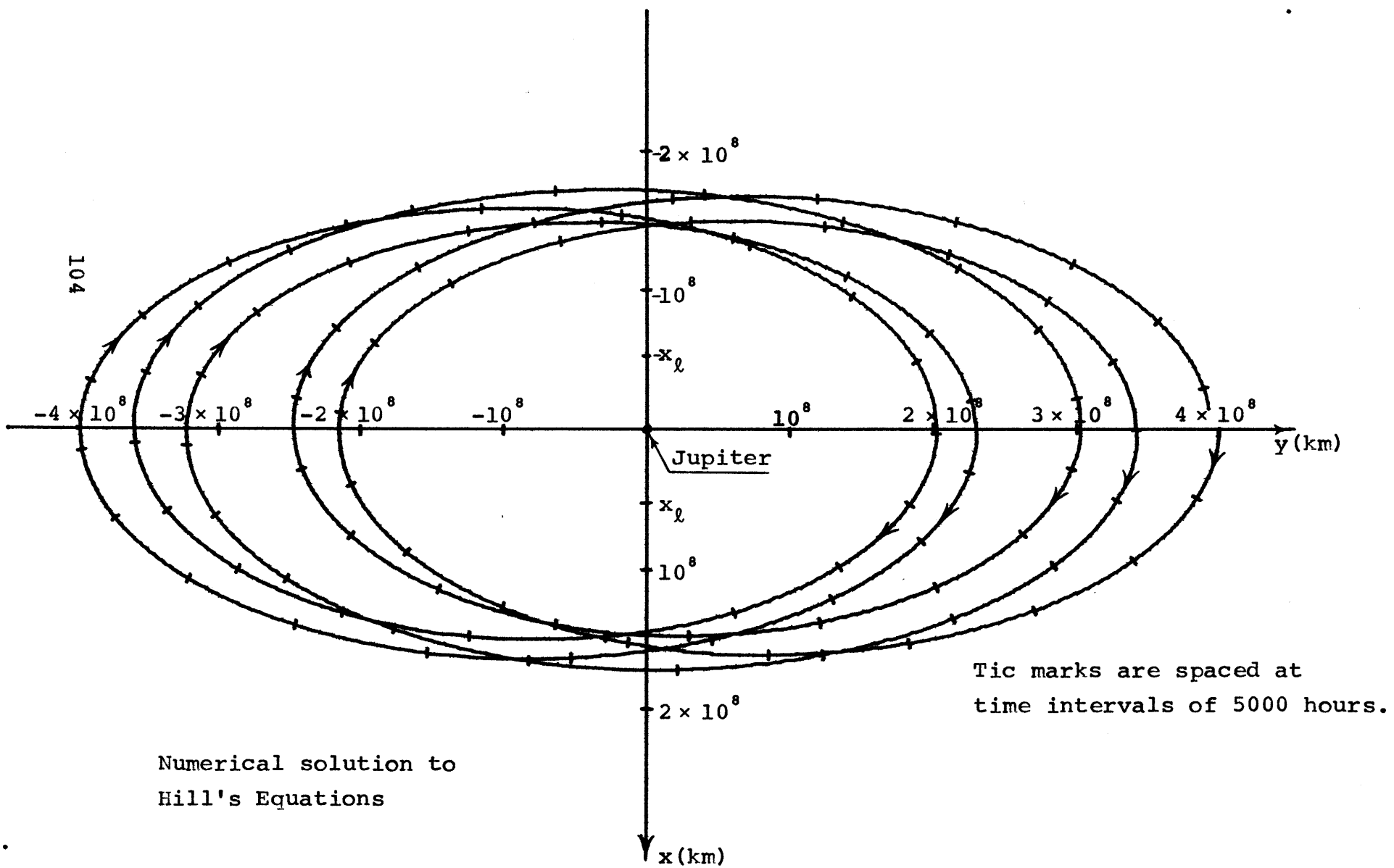
Tic marks are spaced at
time intervals of 5000 hours.

Numerical solution to
Hill's Equations

Figure 5

Case I

$$d_0 = 1.58 \times 10^{11} \, \text{m} \qquad (1.06 \, \text{A.U.})$$

$$\frac{\tilde{y}_0}{d_0} = 0.649$$

$$\frac{x_\ell}{d_0} = 0.3361$$

Quantity	Analysis	Numerical Integration	
		Hill's Equations	Restricted 3-Body
ψ/n	0.1851	0.1937	
$\tilde{y}_0/\tilde{x}_0$	8.102	8.410	
$n'=n(1+k)$	k=0.0782	k=0.0783	

****

Case II

$$d_0 = 4.518 \times 10^{11} \, \text{m} \qquad (3.019 \, \text{A.U.})$$

$$\frac{\tilde{y}_0}{d_0} = 0.662$$

$$\frac{x_\ell}{d_0} = 0.1175$$

Quantity	Analysis	Numerical Integration	
		Hill's Equations	Restricted 3-Body
ψ/n	0.0383	0.0401	
$\tilde{y}_0/\tilde{x}_0$	39.17	38.09	
$n'=n(1+k)$	k=0.00334	k=0.00351	

Table 2

a breakdown in the analysis will not invalidate our basic quali-
tative explanation for the stability of these orbits provided in
the next section.

The last two columns in table 2 permit a comparison of the
orbital parameters resulting from a numerical integration of Hill's
equations with the corresponding parameters resulting from a nu-
merical integration of the restricted three-body equations. It
can be seen that while Hill's equations appear adequate for $d_0 \simeq$
1 A.U. (corresponding to a heliocentric eccentricity of 0.2),
they are not a good approximation to the real situation when $d_0 \simeq$
3 A.U. (corresponding to a heliocentric eccentricity of 0.6).

V. Discussion

At this point a simple physical explanation for the stability of the variation orbit might be welcome in order to clarify what has already been demonstrated both analytically and numerically. In this regard, noting the differences and similarities between the variation orbit and "stationkeeping" orbits is particularly instructive. First consider a third body's variation orbit whose center slightly lags behind a secondary. Then since the third body will be closest to the secondary when it is also in front of the latter, the net perturbing acceleration of the secondary on the third body will be a retarding one. This will "decelerate" the variation orbit (which is now being regarded as an entity in and of itself) and cause its center to migrate inside the secondary's orbit. Consequently, this center must slowly overtake the secondary and move forward. Conversely, if the center of the variation orbit starts out ahead of the secondary, the closest approach will be behind it and the third body's variation orbit will undergo a net acceleration. Then the variation orbit's center will be raised so as to move outside the secondary's orbit and be overtaken by the secondary. Note that the secondary's gravitational perturbations seem to "attract" the variation orbit's center yet "repel" a stationkeeping third body. The reason for this difference lies in the fact that the direction of the secondary's net gravitational acceleration is in the same direction as the displacement of the variation orbit's center, but in the opposite direction for a "stationkeeping" displacement.

References

Alexeyeva, K. N. (1958). Physical properties of stony meteorites and their interpretation in the light of hypotheses regarding the origin of the meteorites (in Russian). Meteoritika 16, 67-77.

Alexeyeva, K. N. (1960). New data on the physical properties of stony meteorites (in Russian). Meteoritika 18, 68-76.

Anders, E. (1964). Origin, age and composition of meteorites. Space Sci. Rev. 3, 583-714.

Anders, E. (1971a). Meteorites and the early solar system. Annual Reviews of Astronomy and Astrophysics 9, 1-34.

Anders, E. (1971b). Interrelations of meteorites, asteroids, and comets. In Physical Studies of Minor Planets (T. Gehrels, Ed.), pp 429-446. NASA SP-267.

Benest, D. (1971). Elliptic restricted problem for Sun-Jupiter: Existence of stable retrograde satellites at large distance. Astron. Astrophys. 13, 157-160.

Berg, O. E., and Gerloff, U. (1970). Orbital elements of micrometeorites derived from Pioneer 8 measurements. J. Geophys. Res. 75, 6932-6939.

Bogard, D. D., Clark, R. S., Keith, J. E., and Reynolds, M. A. (1971). Noble gases and radionuclides in Lost City and other recently fallen meteorites. J. Geophys. Res. 76, 4076-4083.

Brecher, A., Briggs, P. L., and Simmons, G. (1975). The low-temperature electrical properties of carbonaceous meteorites. Earth Planet. Sci. Lett. 28, 37-45.

Chapman, C. R., Morrison, D., and Zellner, B. (1975). Surface
properties of asteroids: A synthesis of polarimetry, radiometry,
and spectrophotometry. Icarus 25, 104-130.

Chebotarev, G. A. (1974). New types of orbits for Trojan aster-
oids. Sov. Astron. 17, 677-679.

Dainty, A. M., Stein, S., and Toksöz, M. N. (1975). Variations
in the number of meteoroid impacts on the moon with lunar
phase. Geophys. Res. Lett. 2, 273-276.

Dohnanyi, J. S. (1971). Fragmentation and distribution of aster-
oids. In Physical Studies of Minor Planets (T. Gehrels, Ed.),
pp 263-295. NASA SP-267.

Dohnanyi, J. S. (1972). Interplanetary objects in review:
Statistics of their masses and dynamics. Icarus 17, 1-48.

Everhardt, P., and Geiss, J. (1964). Meteorite classes and ra-
diation ages. In Isotopic and Cosmic Chemistry (H. Craig,
S. L. Miller, and G. J. F. Wasserburg, Eds.), pp. 452-470.
Amsterdam-London, North-Holland.

Eshleman, V. R. and Gallagher, P. B. (1962). Radar studies of
15th-magnitude meteors. Astron. J. 67, 245-248.

Gault, D. E., Shoemaker, E. M., and Moore, H. J. (1963). Spray
ejected from the lunar surface by meteoroid impact. NASA TN
D-1767.

Hawkins, G. S. (1962). Radar determination of meteor orbits.
Astron. J. 67, 241-244.

Hénon, M. (1970). Numerical exploration of the restricted prob-
lem. VI. Hill's case: Non-periodic orbits. Astron. Astro-
phys. 9, 24-36.

Herzog, G. F. and Anders, E. (1971). Radiation age of the Norton County meteorite. *Geochim. Cosmochim. Acta* 35, 239-244.

Icke, V. (1973). Distribution of the angular velocities of the asteroids. *Astron. Astrophys.* 28, 441-445.

Jacchia, L. G. (1963). Meteors, meteorites and comets; Inter-relations. In *Moon, Meteorites and Comets* (B. M. Middlehurst and G. P. Kuiper, Eds.), pp. 774-798. Univ. of Chicago Press, Chicago, Ill.

Lowrey, B. E. (1971). Orbital evolution of Lost City meteorite. *J. Geophys. Res.* 76, 4084-4089.

McCord, T. B. and Gaffey, M. J. (1974). Asteroids: Surface composition from reflection spectroscopy. *Science* 186, 352-355.

McCrosky, R. E. (1968). Orbits of photographic meteors. *Smithson. Astrophys. Obs. Spec. Rept. No.* 252.

Öpik, E. J. (1951). Collision probabilities with the planets and the distribution of interplanetary matter. *Proc. Roy. Irish Acad.* 54, 165-199.

Paddack, S. J. (1969). Rotational bursting of small celestial bodies: Effects of radiation pressure. *J. Geophys. Res.* 74, 4379-4381.

Paddack, S. J. and Rhee, J. W. (1975). Rotational bursting of interplanetary dust particles. *Geophys. Res. Lett.* 2, 365-367.

Peterson, C. A. (1966). Use of thermal reradiative effects in spacecraft attitude control. M. S. thesis, Massachusetts Institute of Technology, Cambridge, Mass.

Peterson, C. A. (1975). A major perturbing force on small
$(1 < R < 10^4$ cm) solar system bodies: The Yarkovsky effect.
Bull. Am. Astron. Soc. 7, 376.

Radzievsky, V. V. (1952). On the influence of an anisotropic
reemission of solar radiation on the orbital motion of aster-
oids and meteorites (in Russian). Astronomicheskii Zhurnal
29, 162-170.

Radzievsky, V. V. (1954). A mechanism for the disintegration of
asteroids and meteorites. Doklady Akademie Nauk SSSR 97, 49-52.

Robertson, H. P. (1937). Dynamical effects of radiation in the
solar system. Monthly Notices Roy. Astron. Soc. 97, 423-438.

Sparrow, J. G. (1975). Solar radiation induced rotational burst-
ing of interplanetary particles. Geophys. Res. Lett. 2, 255-
257.

Wasson, J. T. (1974). Meteorites. Springer-Verlag, Berlin-
Heidelberg-New York.

Wetherill, G. W. and Williams, J. G. (1968). Evaluation of the
Apollo asteroids as sources of stone meteorites. J. Geophys.
Res. 73, 635-648.

Wetherill, G. W. (1969). Relationships between orbits and sources
of chondritic meteorites. In Meteorite Research (P. M. Millman
Ed.), pp. 573-589. Reidel, Dordrecht.

Wetherill, G. W. (1971). Cometary versus asteroidal origin of
chondritic meteorites. In Physical Studies of Minor Planets
(T. Gehrels, Ed.), pp. 447-460. NASA SP-267.

Wetherill, G. W. (1974). Solar system sources of meteorites and
    large meteoroids. Annual Review of Earth and Planetary
    Sciences 2, 303-331.

Williams, J. G. (1969). Secular perturbations in the solar
    system. Ph. D. thesis, University of California, Los Angeles.

Williams, J. G. (1972). As reported on page 142 of Wasson (1974).

Williams, J. G. (1973). Meteorites from the asteroid belt?
    American Geophysical Union Transactions 54, 233.

Williams, J. G. (1975). The resonant orbit of the Lost City
    meteorite. J. Geophys. Res. 80, 2914-2916.